

RESEARCH PAPER



Mitochondrial autophagy and cell survival is regulated by the circadian *Clock* gene in cardiac myocytes during ischemic stress

Inna Rabinovich-Nikitin^a, Mina Rasouli^b, Cristine J. Reitz^b, Illana Posen^a, Victoria Margulets^a, Rimpay Dhingra^a, Tarak N. Khatua^b, James A. Thliveris^c, Tami A. Martino^{b,*}, and Lorrie A. Kirshenbaum^{a,d,*}

^aDepartment of Physiology and Pathophysiology, The Institute of Cardiovascular Sciences, St. Boniface Hospital Albrechtsen Research Centre, Winnipeg, Manitoba, Canada; ^bCentre for Cardiovascular Investigations, Biomedical Sciences, University of Guelph, Guelph, Ontario, Canada; ^cDepartment of Human Anatomy and Cell Science, Rady College of Medicine, Max Rady Faculty of Health Sciences, University of Manitoba, Winnipeg, Manitoba, Canada; ^dDepartment of Pharmacology and Therapeutics, Rady College of Medicine, Max Rady Faculty of Health Sciences, University of Manitoba, Winnipeg, Manitoba, Canada

ABSTRACT

Cardiac function is highly reliant on mitochondrial oxidative metabolism and quality control. The circadian *Clock* gene is critically linked to vital physiological processes including mitochondrial fission, fusion and bioenergetics; however, little is known of how the *Clock* gene regulates these vital processes in the heart. Herein, we identified a putative circadian CLOCK-mitochondrial interactome that gates an adaptive survival response during myocardial ischemia. We show by transcriptome and gene ontology mapping in CLOCK $\Delta 19/\Delta 19$ mouse that *Clock* transcriptionally coordinates the efficient removal of damaged mitochondria during myocardial ischemia by directly controlling transcription of genes required for mitochondrial fission, fusion and macroautophagy/autophagy. Loss of *Clock* gene activity impaired mitochondrial turnover resulting in the accumulation of damaged reactive oxygen species (ROS)-producing mitochondria from impaired mitophagy. This coincided with ultrastructural defects to mitochondria and impaired cardiac function. Interestingly, wild type CLOCK but not mutations of CLOCK defective for E-Box binding or interaction with its cognate partner ARNTL/BMAL-1 suppressed mitochondrial damage and cell death during acute hypoxia. Interestingly, the autophagy defect and accumulation of damaged mitochondria in CLOCK-deficient cardiac myocytes were abrogated by restoring autophagy/mitophagy. Inhibition of autophagy by ATG7 knockdown abrogated the cytoprotective effects of CLOCK. Collectively, our results demonstrate that CLOCK regulates an adaptive stress response critical for cell survival by transcriptionally coordinating mitochondrial quality control mechanisms in cardiac myocytes. Interdictions that restore CLOCK activity may prove beneficial in reducing cardiac injury in individuals with disrupted circadian CLOCK.

Abbreviations: ARNTL/BMAL1: aryl hydrocarbon receptor nuclear translocator-like; ATG14: autophagy related 14; ATG7: autophagy related 7; ATP: adenosine triphosphate; BCA: bovine serum albumin; BECN1: beclin 1, autophagy related; bHLH: basic helix-loop-helix; CLOCK: circadian locomotor output cycles kaput; CMV: cytomegalovirus; COQ5: coenzyme Q5 methyltransferase; CQ: chloroquine; CRY1: cryptochrome 1 (photolyase-like); DNM1L/DRP1: dynamin 1-like; EF: ejection fraction; EM: electron microscopy; FS: fractional shortening; GFP: green fluorescent protein; HPX: hypoxia; i.p.: intraperitoneal; I-R: ischemia-reperfusion; LAD: left anterior descending; LVIDd: left ventricular internal diameter diastolic; LVIDs: left ventricular internal diameter systolic; MAP1LC3/LC3: microtubule-associated protein 1 light chain 3; MFN2: mitofusin 2; MI: myocardial infarction; mPTP: mitochondrial permeability transition pore; NDUFA4: Ndufa4, mitochondrial complex associated; NDUFA8: NADH: ubiquinone oxidoreductase subunit A8; NMX: normoxia; OCR: oxygen consumption rate; OPA1: OPA1, mitochondrial dynamin like GTPase; OXPHOS: oxidative phosphorylation; PBS: phosphate-buffered saline; PER1: period circadian clock 1; PPARGC1A/PGC-1 α : peroxisome proliferative activated receptor, gamma, coactivator 1 alpha; qPCR: quantitative real-time PCR; RAB7A: RAB7, member RAS oncogene family; ROS: reactive oxygen species; RT: room temperature; shRNA: short hairpin RNA; siRNA: small interfering RNA; TFAM: transcription factor A, mitochondrial; TFEB: transcription factor EB; TMRM: tetra-methylrhodamine methyl ester perchlorate; WT: wild -type; ZT: zeitgeber time

ARTICLE HISTORY

Received 2 December 2020
Revised 28 May 2021
Accepted 1 June 2021



KEYWORDS

Autophagy; clock; metabolism; mitochondrion; myocardial infarction


Introduction

The heart is among the most metabolically demanding organs in the body, requiring a constant and continual supply of ATP to sustain normal cellular processes.

A mismatch between energy supply and demand invariably leads to cardiac dysfunction and heart failure. Mitochondria constitute more than a third of the total cardiac mass and provide the primary source of ATP from the oxidation

CONTACT Lorrie A. Kirshenbaum  LKirshenbaum@sbc.ca  Institute of Cardiovascular Sciences, St. Boniface General Hospital Research Centre, Rm. 3016, 351 Taché Avenue, Winnipeg, Manitoba R2H 2A6, Canada

*These authors contributed equally to this work

 Supplemental data for this article can be accessed [here](#).

(OXPHOS) of glucose and fatty acids; that varies predictably in response to cardiac workload across the 24-h day and night cycle [1–4]. Abnormalities in mitochondrial metabolism, resulting from excessive reactive oxygen species (ROS) production, profoundly influence mitochondrial health in cardiometabolic disorders such as obesity, diabetes and myocardial infarction (MI) [5]. Mitochondrial fitness in cardiac myocytes is achieved through coordinated actions of mitochondrial quality control, dynamics (fission/fusion) and selective macroautophagy/autophagy [6]. The circadian is highly conserved throughout evolution and found in almost every cell type, including cardiac myocytes (reviewed in [7]). Ostensibly, the circadian mechanism allows the cell to respond to environmental cues such as nutrient stress or reduced oxygen availability such as imposed during ischemia or hypoxic stress [8]. The circadian mechanism consists of a transcriptional-translational feedback loop that oscillates with a periodicity of 24 h and coincides with the day-light and night-dark cycle. The rhythmic oscillations of Circadian-controlled output genes underlie the diurnal variation of many key physiological processes including blood pressure, heart rate, and metabolism, [reviewed in [7,9,10]. At the molecular level, the circadian mechanism is comprised of a positive loop consisting of the basic helix-loop-helix (bHLH) transcription factors CLOCK (circadian locomotor output cycles kaput) and ARNTL/BMAL1 (aryl hydrocarbon receptor nuclear translocator-like 1). Upon activation, heterodimers of CLOCK and ARNTL are recruited to E-box elements of circadian target genes *Per1* (period circadian clock 1) and *Per2*, and *Cry1* (cryptochrome 1 (photolyase-like)) and *Cry2*, which comprise the negative arm of the feedback loop and inhibit transcription driven by CLOCK-ARNTL [11]. A stabilizing loop that includes the nuclear orphan receptors NR1D1/REV-ERB and RORA/ROR α provides an additional level of circadian control through their reciprocal regulation of *ARNTL* [reviewed in [7,11].

Molecular dissection of circadian feedback loops has revealed an extensive bi-directional connection between the circadian mechanism in tissues such as the heart and transcription factors involved in mitochondrial metabolism and mitochondrial quality control [12–14]. Furthermore, loss of *ARNTL* is linked to cardiac developmental abnormalities and cardiac hypertrophy [15]. Indeed, circadian misalignment, commonly seen with jet lag or shift work, has been associated with metabolic dysregulation [8,16–18] and greater incidence of cardiac injury following myocardial infarction [19]. The underlying mechanisms for this phenomenon remain unknown. It also remains undetermined whether the circadian core regulatory genes such *Clock* impinge on vital cellular processes such as mitochondrial quality control and bioenergetics that are crucial for cardiac repair after ischemic injury. Since several genes required for mitochondrial quality control processes contain E-boxes elements for the *Clock* gene and exhibit diurnal regulation, we posit that the circadian core gene *Clock* may play a central role in regulating these critical processes during cardiac ischemic stress. Herein, we showed that several

genes required for mitochondrial quality control, dynamics and bioenergetics in cardiac myocytes were transcriptionally controlled by *Clock*. We further showed that impaired autophagy and mitochondrial quality control mechanisms in *Clock* deficiency exacerbated cardiac injury during acute myocardial ischemia. Our findings highlight a novel signaling pathway that functionally links the circadian core regulator gene *Clock* to mitochondrial fitness during ischemic cardiac stress.

Results

Circadian *Clock* gene disruption impairs cardiac structure and function

Since circadian misalignment such as in shift workers, has been associated with greater incidence of cardiac impairment following myocardial injury, we reasoned that disruption of the circadian core protein, CLOCK, may influence cardiac outcomes following injury by interfering with key cellular processes such as mitochondrial metabolism, bioenergetics, and quality control mechanisms. To explore this possibility, we assessed *Clock* mRNA and protein expression levels in hearts of mice subjected to 45 min coronary artery ligation and 24-h reperfusion. As shown by mRNA and western blot analysis, **Figure 1A, Figure 1B**, a significant reduction in *Clock* mRNA and protein expression level was observed in mice following ischemia-reperfusion (I-R) compared to sham-operated controls.

Based on these findings, we reasoned that circadian misalignment resulting from impaired CLOCK activity may underlie the reported cardiac dysfunction following I-R. To test this possibility, we assessed the impact of I-R on cardiac structure and function in wild-type (WT) mice and mice with disrupted circadian rhythm harboring a deletion mutation in the *Clock* gene (designated CLOCK $\Delta 19/\Delta 19$) [20–24]. As shown by electron microscopy in **Figure 1C**, quantitative analysis revealed that mitochondria of the CLOCK $\Delta 19/\Delta 19$ hearts appeared smaller and less abundant than corresponding WT control hearts. Notably, CLOCK $\Delta 19/\Delta 19$ hearts exhibited greater morphological defects including sarcomere disorganization, fragmented mitochondria with disrupted cristae and presence of cellular debris following I-R than WT mice. These findings are consistent with impaired cellular and mitochondrial quality control mechanisms such as autophagy/mitophagy in the CLOCK $\Delta 19/\Delta 19$ hearts.

We next assessed cardiac function in WT and CLOCK $\Delta 19/\Delta 19$ mice following I-R by measuring the left ventricular internal diameter diastolic (LVIDd), left ventricular internal diameter systolic (LVIDs), ejection fraction (%EF) and fractional shortening (%FS) by echocardiography, 1d after I-R. As shown in **Figure 1D**, pre-ischemic cardiac functional parameters in WT and CLOCK $\Delta 19/\Delta 19$ mice were comparable and not significantly different. However, cardiac function was impaired in the CLOCK $\Delta 19/\Delta 19$ indicated by increased LVIDd and LVIDs, dimensions as well as reduced %EF (56.16 ± 0.51 vs. 62.58 ± 0.37) $p < 0.001$; %FS

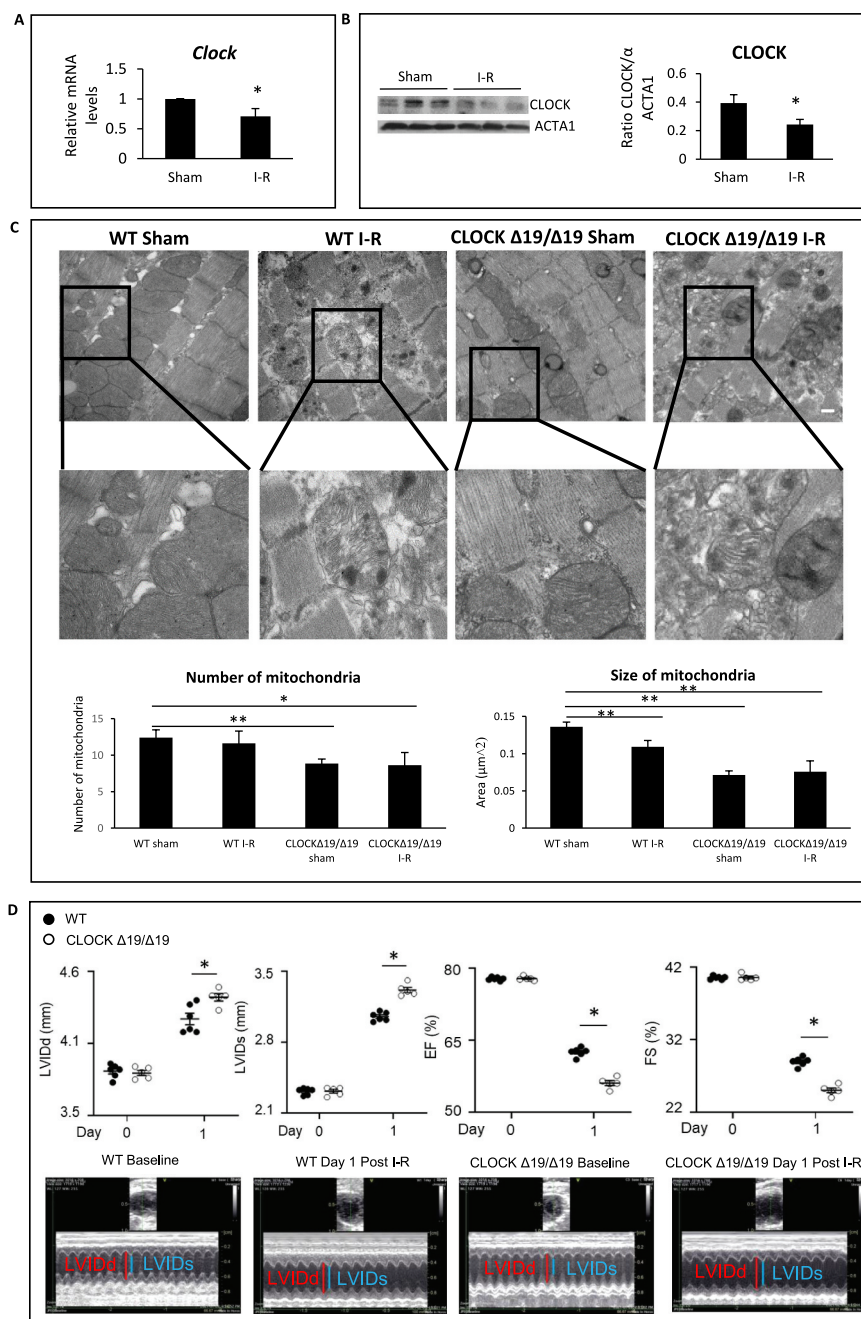


Figure 1. Circadian *Clock* gene disruption impairs cardiac structure and function. (A) *Clock* mRNA expression in murine hearts from sham-operated controls and following ischemia-reperfusion (I-R). (B) *Left panel*; western blot analysis of CLOCK protein expression in murine cardiac muscle in sham-operated controls and following I-R; ACTA1 was used as a loading control; *Right panel* Quantification of western blot analysis from *Left panel*. (C) *Upper*, representative electron micrographs (EM) of murine cardiac muscle from wild-type (WT) and CLOCK $\Delta 19/\Delta 19$ hearts from sham-operated controls and I-R, (see methods for details), *Center panel*, magnified regions of the images, magnification = 500 nm, 19,000X, *Lower panel*, Quantitative analysis for EM images were derived from $n = 4$ randomly selected grids examined at 5800X counting > 80 mitochondria per section, from $n = 3$ sections per mouse heart using $n = 3$ blocks. (D) Echocardiography data for cardiac function in WT and CLOCK $\Delta 19/\Delta 19$ mice pre- and post 24 h following I-R. The *top* histograms represent left ventricular diastolic (LVIDd) dimensions, left ventricular systolic (LVIDs) dimensions, % ejection fraction (% EF) and % fractional shortening (% FS); *bottom*, representative M mode images, data are expressed as mean \pm SEM, * $p < 0.05$, ** $p < 0.01$, $n = 3-5$ mice for each condition tested.

(25.06 ± 0.32 vs. 29.01 ± 0.51), $P < 0.001$), compared to WT mice following I-R (Figure 1D). These findings are consistent with the notion that circadian disruption leads to greater cardiac injury.

Circadian Clock gene disruption impairs cardiac gene expression

Since our *in silico* analysis revealed several genes required for regulating vital quality control processes, mitochondrial

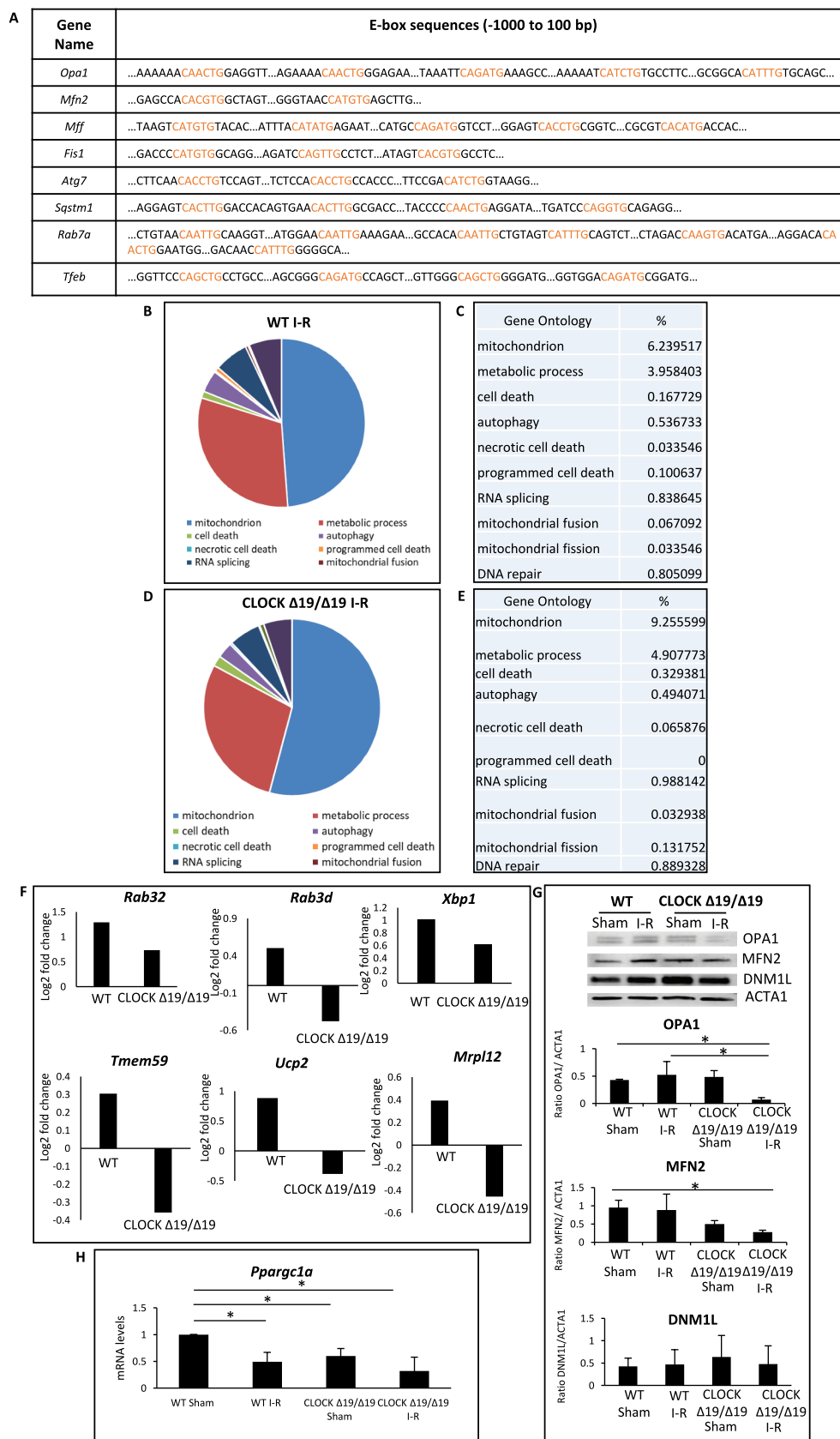


Figure 2. Circadian *Clock* gene transcriptionally targets mitochondrial bioenergetics, dynamics and quality control. (A), E-box elements in *Clock* target genes. Canonical and non-canonical E-box sequences are highlighted in red; (B-E), Pie chart (B and D) represent the most common gene ontology clusters that were altered in response to I-R, tables represent the percentile change of each gene ontology from the total genes in the array (C and E); WT (B and C); CLOCK $\Delta 19/\Delta 19$ (D and E); (F), Histograms represent transcriptomic changes in CLOCK $\Delta 19/\Delta 19$ hearts, including alterations in autophagy, mitochondrial dynamics and mitochondrial energy, *Rab32* $p = 0.04033$; *Rab3d* $p = 0.014746$; *Xbp1*, $p = 8.25E-05$; *Tmem59* $p = 0.014048$; *Ucp2* $p = 0.010898$; *Mrpl12*, $p = 0.001328$; (G), western blot analysis of OPA1, MFN2 and DNM1L protein expression in WT and CLOCK $\Delta 19/\Delta 19$ hearts following I-R, compared to ACTA1 loading control, bottom, quantification of western blot analysis; (H), *PPARGC1A* mRNA expression in WT and CLOCK $\Delta 19/\Delta 19$ hearts following I-R, labels are as described above; data are expressed as mean \pm SEM, * $p < 0.05$, $n = 3-5$ mice hearts for each condition tested.

bioenergetics, and autophagy contained canonical and non-canonical E-box elements for *Clock* (Figure 2A) [25–29], we reasoned that the functional loss of *Clock* activity in CLOCK $\Delta 19/\Delta 19$ mice may have adversely affected these processes and cardiac function following I-R. To test this possibility, we analyzed the cardiac transcriptome by RNA seq analysis in WT, and CLOCK $\Delta 19/\Delta 19$ mice hearts pre- and post I-R *in vivo*. As shown in Figure 2B–E, gene ontology mapping indicated that processes related to mitochondrial metabolism, mitophagy and dynamics were impaired in both the WT and CLOCK $\Delta 19/\Delta 19$ mice hearts following I-R; however, a greater deficit in the gene transcriptome was observed in CLOCK $\Delta 19/\Delta 19$ hearts (Figure 2F). Consistent with these findings, other transcriptomic changes in the CLOCK $\Delta 19/\Delta 19$ hearts included altered expression of genes involved in OXPHOS metabolism, electron transport and mitochondrial biogenesis including *Ndufa8*, *Ndufa4*, *Coq5* (Table S1). In view of this information, we validated the RNA seq data for mitochondrial dynamic proteins, OPA1, MFN2 and DNMI1/DRP-1 as well as the biogenesis factor PPARGC1A/PGC-1 α in the WT and CLOCK $\Delta 19/\Delta 19$ hearts. As shown by western blot analysis in Figure 2G, expression of OPA1, and MFN2, were both decreased in the CLOCK $\Delta 19/\Delta 19$ hearts compared to WT controls. Conversely, DNMI1 expression in the CLOCK $\Delta 19/\Delta 19$ remains unchanged from WT hearts – a finding concordant with the RNA Seq data. Interestingly, a 1.7-fold reduction $p < 0.05$ in the basal expression level of *Ppargc1a* was observed in sham CLOCK $\Delta 19/\Delta 19$ compared to sham WT controls. These findings are consistent with the dependency of *Ppargc1a* expression on *Clock* activity and smaller mitochondria in the CLOCK $\Delta 19/\Delta 19$ hearts. Interestingly, while *PPARGC1A* expression had declined in both the WT and CLOCK $\Delta 19/\Delta 19$ hearts following I-R, the reduction in *PPARGC1A* expression was greater in the CLOCK $\Delta 19/\Delta 19$ (Figure 2H).

CLOCK $\Delta 19/\Delta 19$ promotes mitochondrial dysfunction and cell death in cardiac myocytes

Given that several genes important for mitochondrial dynamics, bioenergetics and autophagy/mitophagy were markedly downregulated in CLOCK $\Delta 19/\Delta 19$ hearts following I-R, to better understand the functional importance of the *Clock* $\Delta 19$ mutation on mitochondrial function and cell viability, we next investigated the impact of *Clock* $\Delta 19$ mutation in cardiac myocytes *in vitro*. As shown in Figure 3A–D, in contrast to vector control cells, cardiac myocytes expressing *Clock* $\Delta 19$ exhibited mitochondrial perturbations including increased ROS production (Figure 3A), loss of mitochondrial membrane potential $\Delta\Psi_m$ (Figure 3B) and increased mitochondrial permeability transition pore (mPTP) opening (Figure 3C). Notably, mitochondrial injury observed in cardiac myocytes expressing the *Clock* $\Delta 19$ was exacerbated during hypoxia.

To further address whether mitochondrial clearance via mitophagy was influenced by impaired *Clock* activity, we monitored mitophagy in cardiac myocytes using the dual fluorescence probe MitoKeima. MitoKeima readily distinguishes unfused mitochondria – lysosomes as (green

fluorescence, neutral pH) or mitochondria fused with lysosomes as (red/yellow fluorescence, acidic pH). The appearance of large red/yellow MitoKeima puncta is indicative of the accumulation of mitophagosomes from disrupted mitochondrial – lysosomal clearance, whereas the presence of smaller green puncta is an index of mitochondrial clearance [30]. Concordant with the mitochondrial damage observed in cardiac myocytes expressing the *Clock* $\Delta 19$, mitochondrial clearance via mitophagy was severely compromised. Indeed, the co-localization signal and size of yellow staining puncta, indicative of impaired mitophagy, were both increased in cardiac myocytes expressing the *Clock* $\Delta 19$ mutant, compared to vector control cells (Figure 3D). In addition, the impaired mitophagy coincided with a marked reduction in cell viability in cells expressing the *Clock* $\Delta 19$ and was further increased during hypoxia (Figure 3E). Together, these findings substantiate our *in vivo* CLOCK $\Delta 19/\Delta 19$ data and support the notion that CLOCK plays a critical role in regulating basal mitochondrial function, mitophagy and cell viability.

CLOCK deficiency provokes mitochondrial perturbations and cell death

To substantiate the importance of CLOCK in the regulation of mitochondrial function and cell viability, we conducted additional experiments in which *Clock* activity was inhibited in cardiac myocytes. For these studies, we used small interfering RNA to knockdown *Clock* activity (*siClock*) in cardiac myocytes *in vitro*. Previously we showed that this approach achieves a knockdown efficiency of 80–85% in post-natal cardiac myocytes [31]. To eliminate off-target effects from the siRNA, we transduced cardiac myocytes with the *Clock* expression vector in the presence of the *siClock* or scrambled interference RNA (scRNA). As shown by western blot analysis in Figure 4A, in contrast to vector control cells, a significant reduction in CLOCK protein expression was observed in cardiac myocytes transduced with *siClock*. This coincided with mitochondrial perturbations that included impaired respiration (Figure 4B), ROS production (Figure 4C), loss of mitochondrial membrane potential $\Delta\Psi_m$ (Figure 4D) and mPTP opening (Figure 4E). Further, knockdown of *Clock* activity resulted in widespread cell death (Figure 4F). Taken together these findings verify the functional importance of *Clock* gene activity on mitochondrial integrity and cell cardiac viability – a finding consistent with the RNA seq data.

CLOCK restores mitochondrial function in cardiac myocytes during hypoxia

To test the significance of CLOCK under physiologically relevant conditions, we investigated the impact of CLOCK in cardiac myocytes under normoxic and hypoxic conditions. Interestingly, as shown in Figure 5A, we observed that endogenous *Clock* mRNA expression oscillated in a reciprocal manner throughout a 24-h period under both normoxic and hypoxic conditions. In contrast to normoxic control cells, a significant reduction in *Clock* mRNA expression was observed in cardiac myocytes subjected to hypoxia that was statistically different from normoxic controls at 18 h

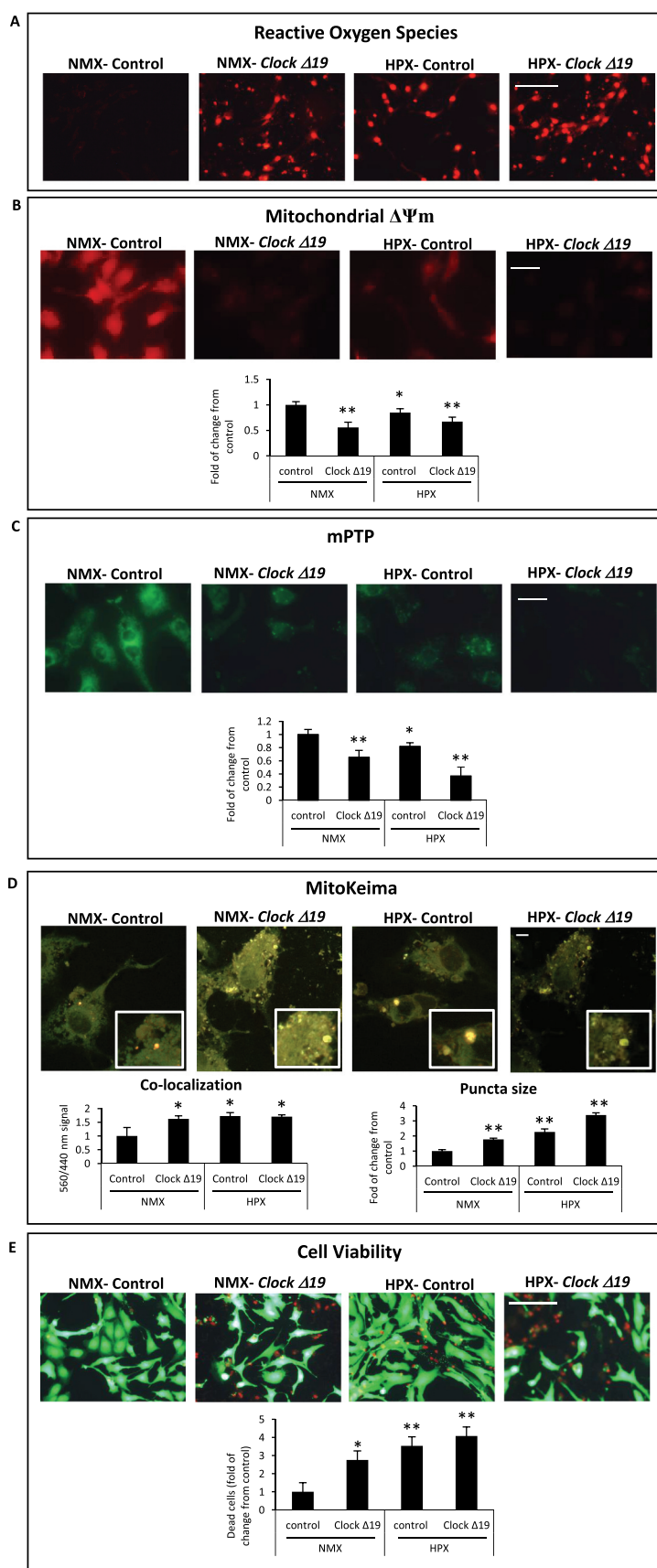


Figure 3. Circadian *Clock Δ19* mutation impairs mitochondrial function, mitophagy and cell viability in cardiac myocytes. Epifluorescence microscopy of cardiac myocytes under normoxic (NMX) or hypoxic (HPX) conditions in the absence and presence of *Clock Δ19* expression vector; (A), mitochondrial reactive oxygen species (ROS) by dihydroethidine (red fluorescence), bar: 100 μ m; (B), mitochondrial membrane potential ($\Delta\Psi_m$) by TMRM (red fluorescence), bar: 20 μ m; (C), mitochondrial permeability transition pore opening (mPTP), (green fluorescence) bar: 20 μ m; see Materials and Methods for details; (D), *Upper*, representative images for MitoKeima staining, as an index of mitophagy in cardiac myocytes under NMX and HPX conditions in the absence and presence of *Clock Δ19* expression vector, bars: 10 μ m. Magnified regions are depicted by the white boxes, green fluorescent puncta demark mitochondria that are unfused with lysosomes (neutral pH), red/yellow

fluorescent puncta demark mitochondria that have fused with lysosomes (acidic pH) indicative of mitophagy. *Bottom* histogram, quantitative analysis for conditions shown above; (E), Cell viability as assessed with vital dyes calcein-AM and ethidium-homodimer-1 to identify the number of live (green) and dead (red) cells, respectively, bar: 100 μ m, see methods for details; data are expressed as mean \pm SEM. * $p < 0.05$; ** $p < 0.01$, $n = 3-4$ independent myocyte isolations, counting >200 cells for each condition tested.

(Figure 5B). Based on these findings, we studied the connection between mitochondrial function and *Clock* gene activity during hypoxia at the 18-h time point. As shown in Figure 5C, in contrast to normoxic control cells, mitochondrial aspect ratio, indicative of increased mitochondrial fission was observed in cardiac myocytes subjected to hypoxia. This was accompanied by a concomitant decline in mitochondrial respiration (Figure 5D), increased ROS production (Figure 5E), loss of mitochondrial membrane potential $\Delta\Psi_m$ (Figure 5F) and mPTP opening (Figure 5G). Moreover, a significant decline in mitochondrial fusion proteins, OPA1 and MFN2 was observed in cardiac myocytes subjected to hypoxia (Figure 5H). Importantly, overexpression of CLOCK restored mitochondrial dynamic proteins, mitochondrial aspect ratio, and bioenergetics (Figure 5). These findings substantiate that CLOCK regulates vital cellular and mitochondrial processes in cardiac myocytes during hypoxia.

CLOCK restores autophagy in cardiac myocytes during hypoxia

Since RNA seq analysis revealed that several genes important for autophagy regulation are putative transcriptional targets of *Clock*, we next investigated whether autophagy gene expression and autophagic clearance were influenced by CLOCK in cardiac myocytes subjected to hypoxia. As shown in Figure 6A–D, in contrast to normoxic controls, a marked reduction in mRNA expression of autophagy genes *Atg7*, *Tfeb*, *Sqstm1/p62* and *Rab7a* was observed in cardiac myocytes subjected to hypoxia. Further, as shown by western blot analysis (Figure 6E), hypoxia-induced decline in autophagy gene expression coincided with a reduction in BECN1 and ATG14 protein levels. Importantly, the hypoxia-induced decrease in autophagy gene and protein expression was restored to normoxic control levels in cardiac myocytes expressing CLOCK Figure 6A–E. This is further substantiated by the *Clock*-dependent increase in *Tfeb* promoter activity in hypoxic cardiac myocytes expressing *Clock* (Figure S1).

To verify that restoring autophagy gene expression with exogenous *Clock* rescued autophagic clearance, we monitored autophagy flux in cardiac myocytes subjected to hypoxia using the autophagy reporter GFP-LC3 in the absence and presence of chloroquine (CQ). As shown by epifluorescence microscopy (Figure 6F), under normoxic conditions, the number of GFP-LC3 puncta was significantly increased in cardiac myocytes expressing *Clock* and was increased further in cells treated with CQ. These findings confirm that autophagy was functionally operational and activated by CLOCK in cardiac myocytes. Interestingly, the number of GFP-LC3 puncta was only marginally increased in cardiac myocytes during hypoxia, indicating that autophagy was stalled. This finding is consistent with the inhibition of autophagy gene expression in cardiac myocytes during hypoxia. However, the number of

GFP-LC3 staining puncta in hypoxic cardiac myocytes was significantly increased in cells expressing *Clock* and was increased in the presence of CQ. The ability of CLOCK to restore autophagic flux in cardiac myocytes during hypoxia corresponded with and an increase in mitochondrial clearance as demonstrated by decreased co-localization signal and size of Mitokemia puncta, indicative of increased mitophagy (Figure S2A). Concordantly, the increased mitochondrial clearance was accompanied by a corresponding decrease in mitochondrial mass as indicated by a decline in ratio between mitochondrial transcription factor *Tfam* and *Rpl32* (Figure S2B). Moreover, *Ppargc1a* gene expression indicative of mitochondrial biogenesis was markedly increased in cardiac myocytes expressing *Clock* (Figure S2C), consistent with the increased oxidative capacity in *Clock*-expressing cells. These findings demonstrate that mitochondrial clearance and biogenesis are regulated by *Clock* gene activity.

To further investigate the impact of CLOCK on autophagic flux, we investigated whether inhibiting autophagy would interfere with the ability of CLOCK to activate autophagy. For these studies, we inhibited autophagy using an adenovirus encoding shRNA directed against *Atg7* (Ad-shAtg7). As shown in Figure 6F, the ability of CLOCK to activate autophagy was suppressed by *Atg7* knockdown – verifying that autophagy activation was CLOCK-dependent. Furthermore, the ability of CLOCK to rescue cell death during hypoxia was abrogated by *Atg7* knockdown (Figure 6G). These findings support our contention that the survival properties conferred by CLOCK require autophagy/mitophagy activation.

Clock gene transcription regulates mitochondrial bioenergetics, mitophagy and cell survival during hypoxia

To verify whether the transcriptional properties of *Clock* are necessary and sufficient for rescuing mitochondrial autophagy and cell viability, we next assessed the impact of WT *Clock* and mutations of the *Clock* gene within the bHLH hydrophobic core (CLOCK^{L57E}) that render *Clock* defective for E-box binding, or within the PAS domain that destabilizes its heterodimerization with ARNTL (CLOCK^{V315R}), or *Clock* mutant that disrupts both E-box binding and ARNTL interactions (CLOCK^{L57E/L113E/W284}, designated, CLOCK 3xMut) [32], depicted in Figure 7A. As shown in Figure 7B by confocal fluorescence microscopy, in contrast to normoxic control cells which exhibited smaller green staining Mitokemia puncta indicating mitochondria were not fused with lysosomes, we detected a significant increase in the number of large red/yellow puncta in cardiac myocytes subjected to hypoxia, consistent with impaired mitophagy. In contrast, however, the number and size of red/yellow puncta in cardiac myocytes subjected to hypoxia was significantly decreased in cardiac myocytes expressing WT *Clock*. Indeed, cardiac

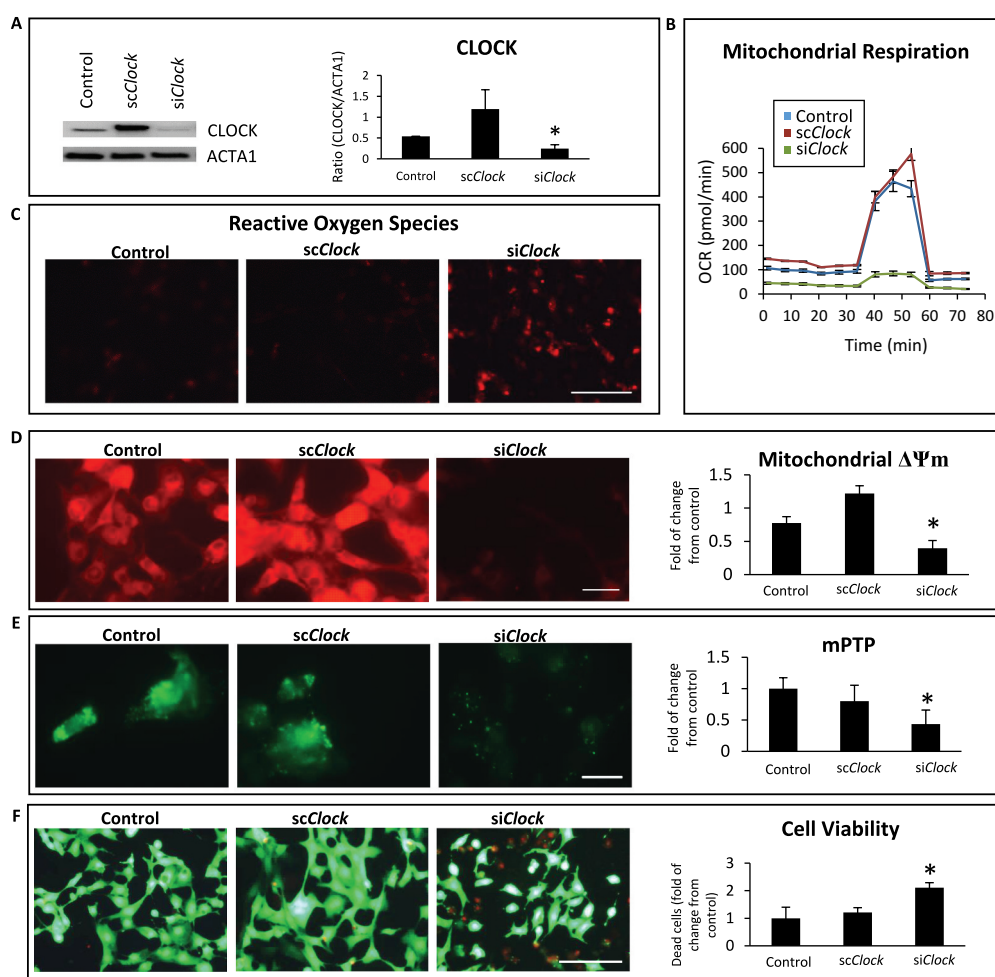


Figure 4. *Clock* knockdown disrupts mitochondrial function and cell viability. (A); Top left, western blot analysis of CLOCK protein expression in post-natal cardiac myocytes. Cardiac myocytes were transfected with vector alone (control) or with the *Clock* expression vector along with short-hairpin RNA directed against *Clock* designated (*siClock*) or with *Clock* expression vector along with scrambled siRNA designated (*scClock*); Lower left, ACTA1 for loading control; Right, histogram represents quantitative data for the western blot analysis; (B), Oxygen consumption rate (OCR) in adenovirus-infected control cells AdCMV or cardiac myocytes infected with Ad*Clock* in the presence of *siClock* or *scClock*; (C), epifluorescence microscopy of reactive oxygen species (ROS) by dihydroethidine, bar: 100 μ m; (D), epifluorescence microscopy of mitochondrial membrane potential $\Delta\Psi_m$ by TMRM staining, bar: 20 μ m; (E), Mitochondrial permeability transition pore opening (mPTP), bar: 20 μ m; (F), cell viability, with vital dyes calcein-AM and ethidium-homodimer-1 to identify the number of live (green) and dead (red) cells, respectively, bar: 100 μ m, see methods for details. Histogram represents quantitative data for $\Delta\Psi_m$, mPTP and cell viability, data are expressed as mean \pm SEM from at least $n = 3$ –4 independent myocyte isolations experiments counting >200 cells for each condition tested, * $p < 0.05$.

myocytes expressing exogenous WT *Clock* were indistinguishable from normoxic control cells with respect to mitophagy, indicating that the mitochondrial clearance was functionally restored in these cells. Conversely, the three *Clock* mutants tested, which were expressed to comparable levels as the wild-type *Clock* (Figure S3), each failed to rescue mitophagy in hypoxic cardiac myocytes. Interestingly, the number, and size of red/yellow MitoKeima puncta was significantly increased with each of the *Clock* mutations tested, indicating that clearance of damaged mitochondria was significantly impaired by the absence of functional *Clock*. Interestingly, the CLOCK 3xMut exhibited the greatest effects on mitophagy impairment even under basal condition, likely reflecting the importance of CLOCK for regulating basal autophagy and mitochondrial clearance. Remarkably, the impaired mitophagy in cardiac myocytes defective for CLOCK activity is consistent with the presence of damaged mitochondria observed in the CLOCK $\Delta 19/\Delta 19$ I-R hearts *in vivo* and

cardiac myocytes expressing the CLOCK $\Delta 19$ *in vitro* (Figure 3). These findings support the notion that autophagy and mitophagy quality control mechanisms are functionally dependent upon *Clock* gene activity. Furthermore, in contrast to WT *Clock*, the *Clock* mutants impaired mitochondrial respiration (Figure 7C), mitochondrial morphology (Figure 7D) and cell viability (Figure 8A) under normoxic conditions that were exacerbated further during hypoxia. In aggregate, these findings demonstrate a novel role for CLOCK as a critical regulator of mitochondrial metabolism, quality control and cell survival of cardiac myocytes.

Discussion

Epidemiologic studies have shown that circadian disruption in humans is associated with increased risk of heart disease and worsened outcomes following cardiac injury, reviewed [7,17,33]. In this report, we provide new compelling evidence

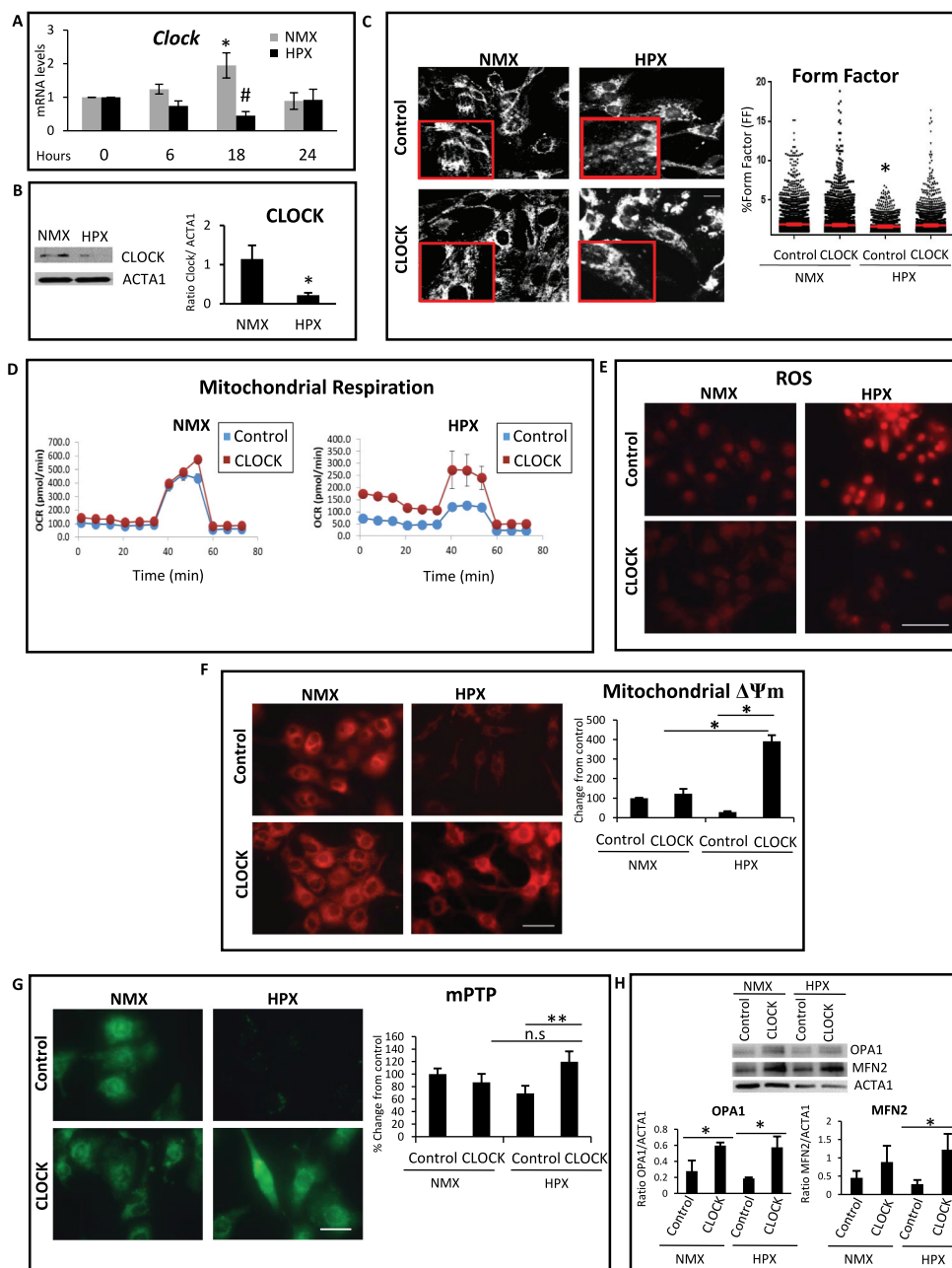


Figure 5. CLOCK restores mitochondrial dynamics, mitochondrial function and mitochondrial bioenergetics during hypoxia. (A). *Clock* mRNA expression in cardiac myocytes is downregulated during hypoxia (HPX) (18 h) compared to normoxic controls (NMX), (B), *Upper left*, western blot analysis of CLOCK protein expression in cardiac myocytes during hypoxia (HPX) of 18 h compared to normoxia (NMX); *Lower left*, ACTA1 as a loading control; *Right*, histogram is quantitative data for the western blot analysis. (C), *Left*, Representative epifluorescence images of cardiac myocytes stained for mitochondrial HSPD1 to assess mitochondrial morphology aspect ratio, bar: 10 μ m, magnified regions are depicted in red boxes, *Right*, quantitative data of mitochondrial morphology is displayed as mitochondrial form factor, (FF), as an index of mitochondrial fusion and fission, lower FF values are indicative of mitochondrial fission relative to control; (D), mitochondrial oxygen consumption rate (OCR) in cardiac myocytes under NMX and HPX conditions, viral control AdCMV (blue box) or AdClock (red box); (E), Epifluorescence microscopy of cardiac myocytes under normoxic (NMX) or hypoxic (HPX) conditions, assessed for mitochondrial reactive oxygen species (ROS) by dihydroethidine (red), bar: 100 μ m; (F), mitochondrial membrane $\Delta\Psi_m$ by TMRM (red), bar: 20 μ m; Histogram represents quantitative data for panel F; (G), mitochondrial permeability transition pore opening (mPTP), (green fluorescence) bar: 20 μ m; Histogram represents quantitative data for panel G; (H) *Upper*, western blot analysis for OPA1 and MFN2 protein expression in cardiac myocytes during normoxia (NMX) and hypoxia (HPX) at 18 h; *Lower*, Histogram represents quantitative analysis for Panel H; see Materials and Methods for details; data are expressed as mean \pm SEM. *# p < 0.05; ** p < 0.01, n.s.- non significant, n = 3–4 independent myocyte isolations, counting >200 cells for each condition tested for Panels C, F–H.

that the circadian *Clock* gene regulates mitochondrial fitness by transcriptionally controlling mitochondrial dynamics, bioenergetics and quality control processes in cardiac myocytes. Our results reveal a novel link between the *Clock* gene activity and cardiac cell survival. We show that loss of *Clock*

gene activity *in vitro* and *in vivo* results in a greater cardiac injury and ventricular dysfunction from impaired activation of autophagy/mitophagy, mitochondrial bioenergetics and dynamics. Since defects in mitochondrial function have been associated with necrotic cell death and cardiac injury

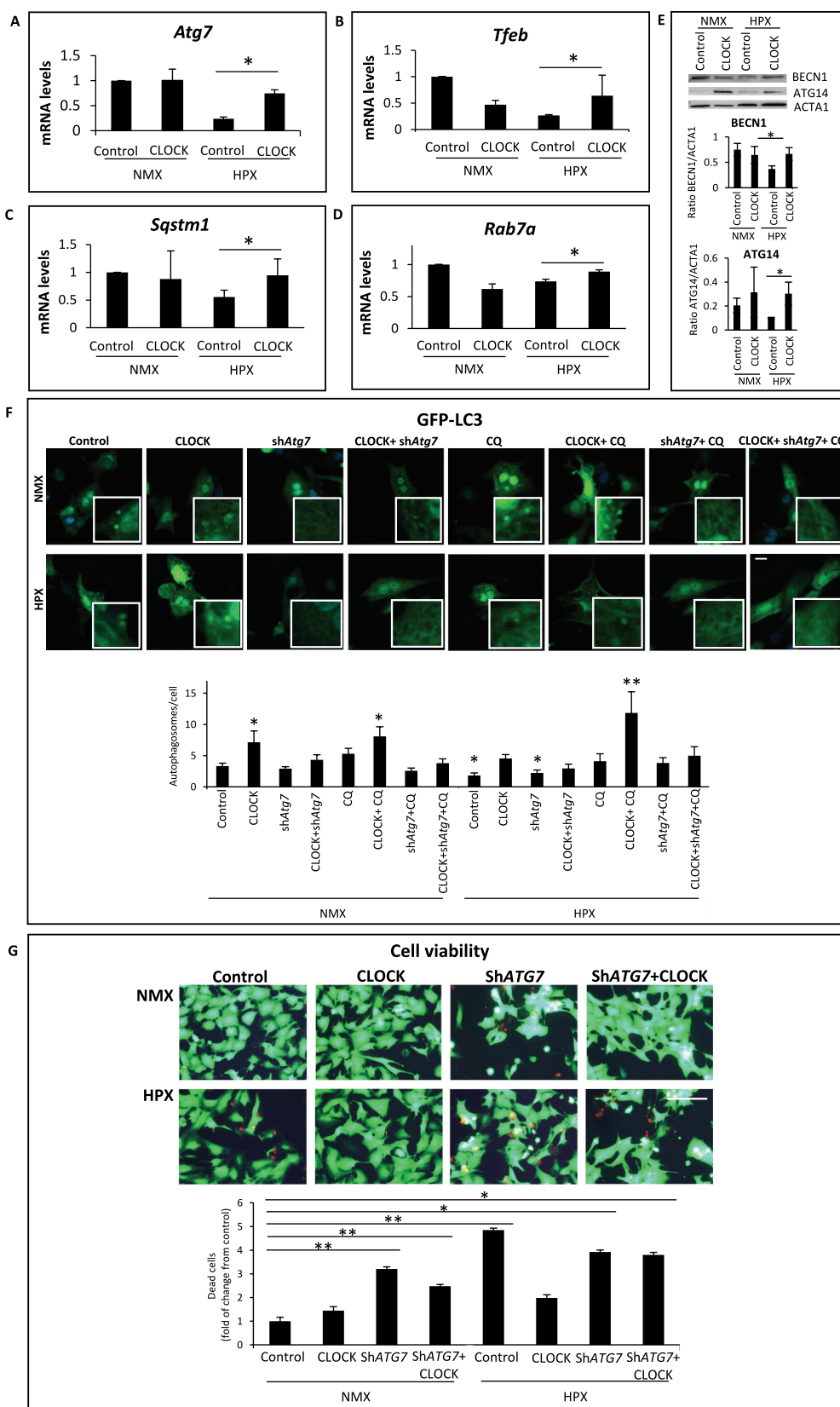


Figure 6. CLOCK restores autophagy gene expression and cell viability during hypoxia. (A-D), mRNA expression levels of autophagic genes in normoxic (NMX) and hypoxic (HPX) cardiac myocytes in the absence and presence of control adenovirus CMV (AdCMV) or AdClock, mRNA levels were normalized to *Rpl32*; (E), Top, western blot analysis of BECN1 and ATG14 protein expression in NMX and HPX cardiac myocytes in the absence and presence of AdCMV or AdClock. Lower panel, histogram represents quantitative data for the western blot, relative to ACTA1 as a loading control, (F), Upper, epifluorescence microscopy of ventricular myocytes expressing autophagy reporter GFP-LC3 (green puncta) and Hoechst 33258 nuclear staining (blue) in the presence of AdCMV (vector control) or, AdClock, or shAtg7 with or without Chloroquine (CQ) to assess autophagic flux under NMX and HPX conditions, bar: 10 μ m, Magnified regions are depicted by the white boxes. Green fluorescent puncta are indicative of increased autophagic flux, Lower, analysis of conditions tested in Upper panel. (G), Left, representative images of MitoKeima

staining, as an index of mitophagy in cardiac myocytes under NMX and HPX conditions 18 h in the absence and presence of AdCMV or Ad*Clock* or sh*Atg7*, bar: 10 μ m. Magnified regions are depicted by the white boxes, green fluorescent puncta demark mitochondria that are not fused with lysosomes (neutral pH), red/yellow fluorescent puncta demark mitochondria that have fused with lysosomes (acidic pH) indicative of mitophagy. *Right*, analysis of conditions tested on left panel; data are expressed as mean \pm SEM. * $p < 0.05$, ** $p < 0.01$, $n = 3-4$ independent myocyte isolations.

[6,34,35], we attributed the greater cell injury and I-R dysfunction in CLOCK $\Delta 19/\Delta 19$ mice to impaired activation of genes important for mitochondrial dynamism and autophagy [36–38].

The notion that impaired mitochondrial quality control processes accounted for the greater cardiac injury observed in the CLOCK $\Delta 19/\Delta 19$ mice is supported by our RNA seq data, which revealed that several genes required for autophagy/mitophagy, as well as mitochondrial dynamism including *Atg7*, *Rab7a*, *Tfeb*, *Sqstm1*, *Mfn2*, *Opa1* and others were markedly downregulated in the CLOCK $\Delta 19/\Delta 19$ hearts. Indeed, disruption of mitochondrial cristae in CLOCK $\Delta 19/\Delta 19$ hearts is consistent with the reduction in MFN2 and OPA1 expression and impaired mitochondrial bioenergetics. Importantly, mitochondrial damage during I-R would activate autophagy/mitophagy to cull damaged mitochondria; however, since autophagic gene expression and autophagy were impaired in the CLOCK $\Delta 19/\Delta 19$ hearts, it is not surprising that autophagic removal of damaged mitochondria in *Clock*-deficient cardiac myocytes was impaired during I-R. These findings highlight the importance of CLOCK in the regulation of autophagy and mitochondrial quality control processes in cardiac myocytes. These findings are further substantiated by the fact that restoring CLOCK activity rescued autophagic gene expression and mitophagy during hypoxia. Based on these findings, we purport that loss of mitochondrial quality control mechanisms, such as seen in the *Clock*-deficient hearts, may underlie the decline in cardiac performance associated with circadian disruption with aging [39].

Cells respond to changes in metabolic demands imposed by hypoxia or ischemic stress [40]. In this study, we provide novel evidence that the circadian *Clock* gene synchronizes mitochondrial turnover, biogenesis and energetics to ensure a healthy pool of mitochondria are available to meet the metabolic needs of the cell. The disruption of a functional *Clock* gene predisposes cardiac myocytes to ischemic/hypoxic stress by preventing activation of critical adaptive mechanisms crucial for maintaining mitochondrial fitness and cell survival. This is evidenced by the mitochondrial fragmentation and increased oxidative injury and cell death. Indeed, changes in mitochondrial architecture from increased fusion have been associated with increased mitochondrial bioenergetics, while mitochondrial fission has been linked impaired oxidative metabolism and mitophagy [41,42]. The fact that mitochondrial dynamics and mitophagy were disrupted in CLOCK $\Delta 19/\Delta 19$ hearts and *Clock*-deficient cardiac myocytes, supports the notion that CLOCK plays a critical role in coordinating mitochondrial dynamics and clearance in the heart. Further, the increased PPARGC1A expression in cardiac myocytes expressing CLOCK is consistent with the increased oxidative capacity and replenishment of mitochondria following mitophagy.

Previous Chip Seq studies have identified several metabolic and mitochondrial genes that contain E-box elements for *Clock* and oscillate in a circadian-dependent manner [43–48]. Indeed, our RNA seq data in cardiac myocytes verify that many of the genes responsible for metabolism, mitochondrial dynamics and quality control are transcriptionally regulated by the *Clock* gene. This is substantiated by our findings that the *Tfeb* promoter activity was activated by CLOCK in cardiac myocytes coincident with an increase in autophagy and mitochondrial clearance, Figure S1. In addition, our discovery of E-box elements within several mitochondrial electron transport genes as well as several genes important for metabolism supports the notion that CLOCK is a master transcriptional regulator that coordinates these processes. Given the fact that the wild type *Clock*, but not mutations of *Clock* defective for DNA-binding to E-box elements or dimerizing with ARNTL, normalized mitochondrial respiration and autophagy gene expression in cardiac myocytes, we speculate that CLOCK may directly serve as a critical regulator mitochondrial function independent of its role in circadian regulation. Further, given that ARNTL was unable to rescue the mitochondrial perturbations and cell death in cardiac myocytes deficient for *Clock* gene activity, would argue that CLOCK and ARNTL have distinct non-overlapping properties with respect to autophagy and mitochondrial quality control in cardiac myocytes. Interestingly, it was recently shown that ARNTL activated DNMI1 and promoted mitochondrial fission in hepatocytes [49]. However, in the present study, we observed that CLOCK activated transcription of mitochondrial fusion proteins, MFN2 and OPA1, yet had no effect on DNMI1 expression or DNMI1 (S616) phosphorylation (I.R.N and L.A.K unpublished data) in cardiac myocytes. These findings suggest that CLOCK and ARNTL may differentially regulate mitochondrial fusion and fission genes in a cell and context-specific. Furthermore, we observed that CLOCK but not ARNTL expression was reduced in cardiac myocytes during ischemia reperfusion *in vivo* or hypoxia *in vitro*. This finding would argue that CLOCK and not ARNTL is important for regulating transcription of autophagy/mitophagy genes in cardiac myocytes. However, this does not preclude the importance or involvement of ARNTL in other forms of cardiac injury, given the recent report highlighting a role for ARNTL in dilated cardiomyopathy [15,50]. Taken together, our study reveals, for the first time, CLOCK as a central regulator of quality control mechanisms and metabolic processes crucial for maintaining oxidative metabolism and cardiac function following I-R. Based on our findings, we propose that the functional impairment of CLOCK activity predisposes cardiac myocytes to oxidative injury and mitochondrial dysfunction during I-R from inadequate mitophagy for culling damaged ROS-producing mitochondria as well as impaired mitochondrial biogenesis for

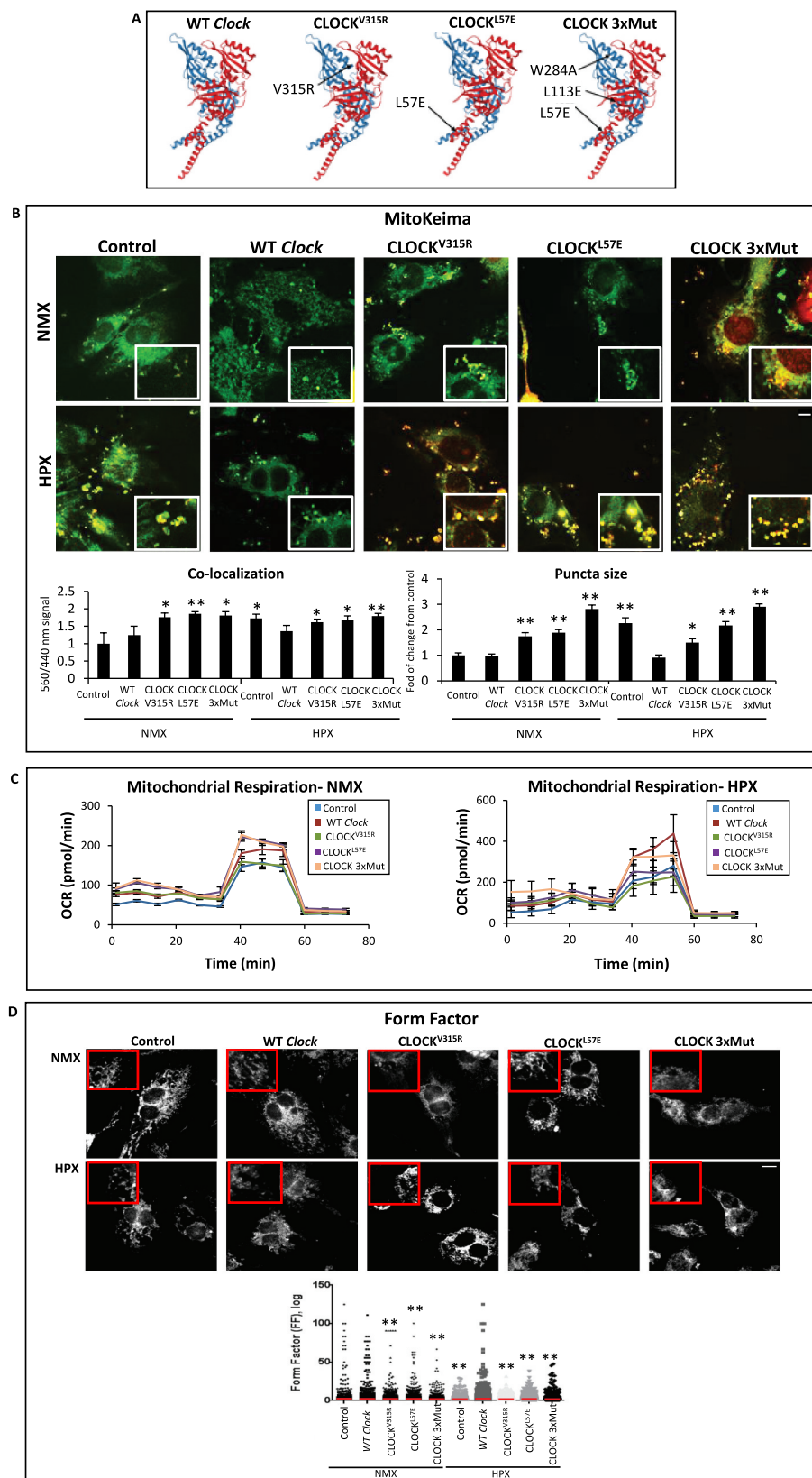


Figure 7. CLOCK rescues mitochondrial bioenergetics and mitophagy in cardiac myocytes. (A), Ribbon structures of wild type (WT) and CLOCK mutants, CLOCK^{V315R}, CLOCK^{L57E}, CLOCK^{L57E/L113E/W284A}, designated as CLOCK 3xMut; blue ribbon represents CLOCK, red ribbon represents ARNTL, as previously reported by [32], Protein Data Bank (PDB) code 4 F3L; (B), *Top*, representative epifluorescence microscopy of MitoKeima staining in cardiac myocytes as an index of mitophagy. Cardiac myocytes expressing MitoKeima reporter under normoxic (NMX) and hypoxic (HPX) conditions 18 h in the presence of *Clock* WT or CLOCK mutants, bar: 10 μ m. Magnified regions are depicted by insets outlined by white boxes, green fluorescence MitoKeima puncta represent mitochondria that unfused with lysosomes (neutral pH), red/yellow fluorescent puncta demark mitochondria that are fused with lysosomes (acidic pH), see methods for details. In contrast to *Clock* WT, each of the CLOCK mutants tested resulted in the accumulation of larger red/yellow MitoKeima puncta indicating that mitophagy and mitochondrial clearance was impaired

(see text for details), *Bottom*, analysis of conditions tested in Upper panel; (C), mitochondrial oxygen consumption rate (OCR) in cardiac myocytes under NMX or HPX conditions in the presence *Clock* WT or *CLOCK* mutants; (D), *Top* Representative epifluorescence images of cardiac myocytes stained for mitochondrial HSPD1 to assess mitochondrial morphology aspect ratio, bar: 10 μ m, magnified regions are depicted in red boxes, *Bottom* quantitative data of mitochondrial morphology is displayed as mitochondrial form factor, (FF), as an index of mitochondrial fusion and fission, lower FF values are indicative of mitochondrial fission relative to control, (E), cell viability of ventricular myocytes stained with vital dyes calcein-AM and ethidium-homodimer-1 to demark the live (green) and dead (red) cells in the absence and presence of *Clock* WT or *CLOCK* mutants, bar: 100 μ m, histogram represents quantitative data for Panel E, data are expressed as mean \pm SEM. * $p < 0.05$; ** $p < 0.01$, $n = 3$ independent myocyte isolations, counting > 200 for each condition tested.

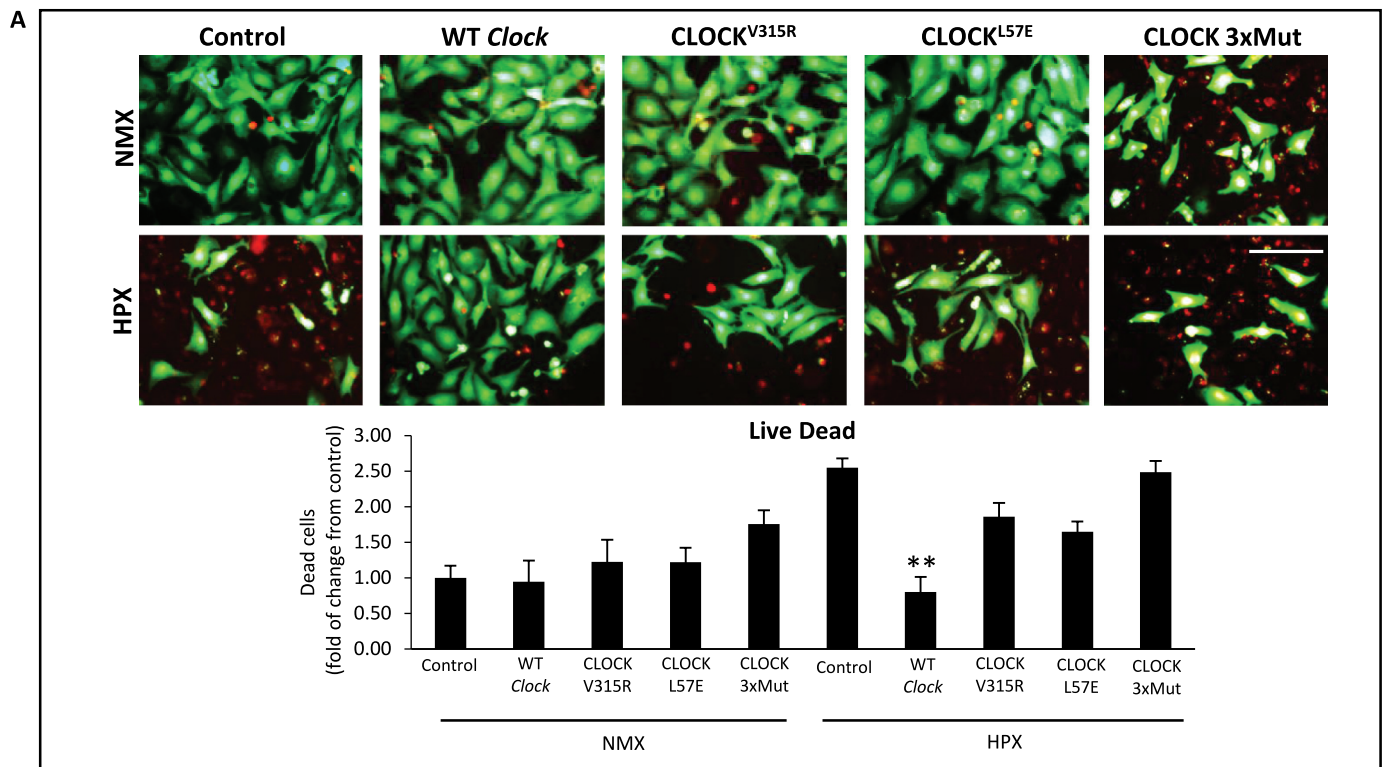


Figure 8. *CLOCK* rescues cell survival in cardiac myocytes. (A), cell viability of ventricular myocytes stained with vital dyes calcein-AM and ethidium-homodimer-1 to demark the live (green) and dead (red) cells in the absence and presence of *CLOCK* WT or *CLOCK* mutants, bar: 100 μ m, histogram represents quantitative data for Panel A, data are expressed as mean \pm SEM. * $p < 0.05$; ** $p < 0.01$, $n = 3$ independent myocyte isolations, counting > 200 for each condition tested.

ATP production (Figure 9). Indeed, the impaired autophagy and uncoupled respiration are consistent with cardiac dysfunction seen in the *CLOCK* $\Delta 19/\Delta 19$ following I-R and *CLOCK* $\Delta 19$ cardiac myocytes during hypoxia. Furthermore, the fact that inhibition of autophagy by *Atg7* knockdown abrogated the ability of *CLOCK* to rescue hypoxia-induced autophagy and cardiac cell death would substantiate the importance of autophagy for the survival properties conferred by *CLOCK*.

In a similar light, our data may explain the increased severity of cardiac injury in individuals with circadian disruption such as shift workers or individuals with sleep disorders, with disrupted *CLOCK* activity [17,18,51]. Hence, interdictions that influence *CLOCK* activity may translate into better cardiac performance in individuals

with circadian *CLOCK* disruption following myocardial infarction.

Materials and methods

Animals

Male homozygote *CLOCK* $\Delta 19/\Delta 19$ and wild-type (WT) littermates on a C57Bl/6 J background used for this study were obtained from Dr. Tami Martino (University of Guelph) [52]. The *CLOCK* $\Delta 19/\Delta 19$ mice encode a mutant *CLOCK* protein that disrupts dimerization with its cognate partner ARNTL1, thereby inhibiting the transcription of circadian controlled genes [20–24]. All animal experiments conducted in this study were approved by animal care committee of

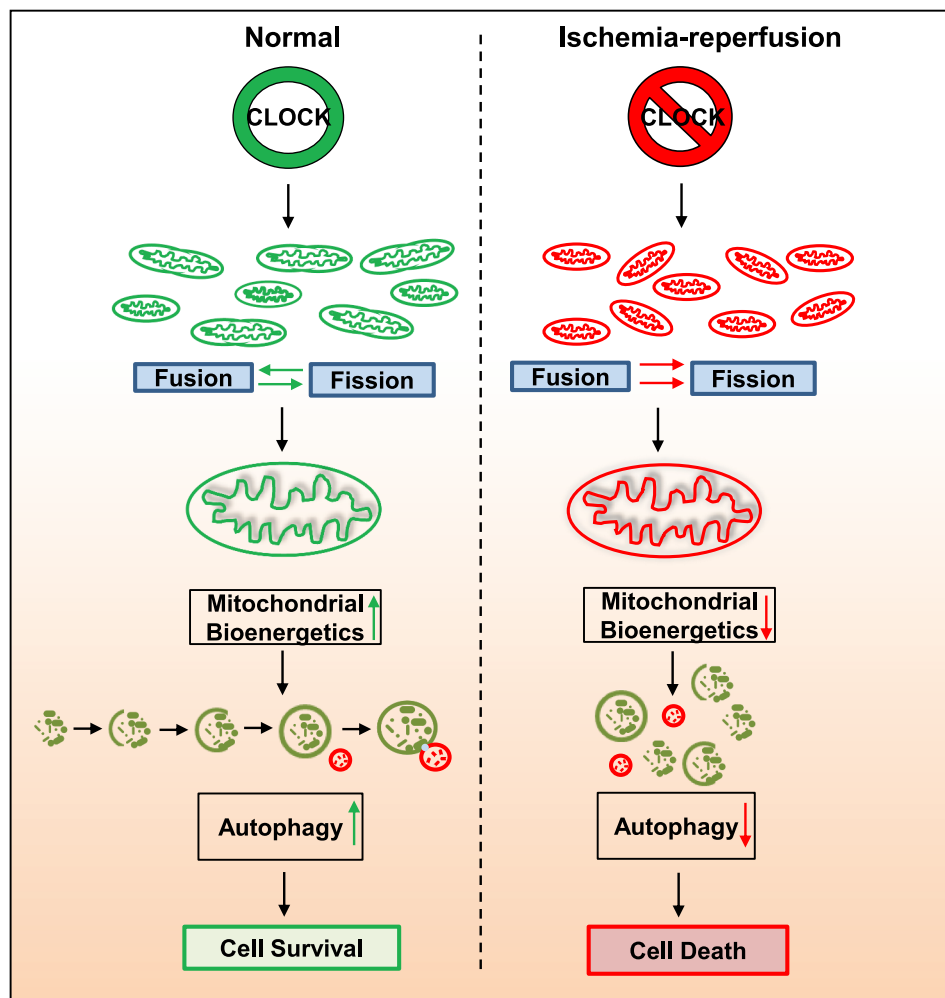


Figure 9. CLOCK Regulates Autophagy and Mitochondrial Quality Control in Cardiac Myocytes. Schematic model for CLOCK regulation of autophagy and mitochondrial quality control. *Left panel*, *Clock* gene expression promotes mitochondrial dynamics, quality control, bioenergetics and cell survival. *Right panel*, disruption of expression of *Clock* gene during ischemia-reperfusion impairs mitochondrial dynamics, quality control and bioenergetics, resulting in cell death.

University of Manitoba as well as by University of Guelph and are in accordance with the guidelines laid for protection of animals used for scientific purposes by Canadian Council for Animal Care, directive 2010/63/EU, and National Institutes of Health (NIH). Animals were housed at an animal facility with standard laboratory conditions, 12–12 h light-dark cycle. Rodent chow (Envigo, 2914) and water were provided *ad libitum*.

Ischemia-reperfusion procedure

All surgeries were performed within 1–4 h after lights on to avoid confounding circadian effects (zeitgeber time (ZT) 01–04). Male C57Bl/6 J and CLOCK $\Delta 19/\Delta 19$ mice were anesthetized with 3.5% isoflurane, intubated, and ventilated (Harvard Apparatus, Model 687). Prior to surgical incision, animals were administered a local subcutaneous injection of a 50:50 mix of bupivacaine (1.5 mg/kg) and lidocaine (3 mg/kg). Mice were then subjected to surgical ligation of the left anterior descending (LAD) coronary artery. To do this, a left-sided incision was made in the third intercostal space to view the

heart and the pericardium was gently dissected to expose the LAD coronary artery. A silk 7–0 suture was passed underneath the LAD at 1 mm below the edge of the left auricle and a piece of PE-10 tubing, approximately 5 mm in length, was placed over the LAD. The suture was tied around the tubing to ligate the LAD for a 45-min ischemic period. The chest and skin were then temporarily closed, with a sterile cloth placed over the incision site. After 45 min, the incision site was reopened and the tubing and suture were removed allowing the LAD to reperfuse. The chest and skin were then closed with silk 6–0 suture. Sham controls underwent the same procedure without ligation of the LAD coronary artery. Mice were administered buprenorphine (0.1 mg/kg) analgesia upon awakening and again at 8 h, and were sacrificed at 24 h post-operation.

Basic RNA-seq data processing

After 24 h of reperfusion, mice were anesthetized and hearts were excised, rinsed in phosphate-buffered saline (PBS; 10x [80 g NaCl, 2 g KCl, 11.5 g $\text{Na}_2\text{HPO}_4 \cdot 7\text{H}_2\text{O}$, 2 g

KH_2PO_4 , pH 7.4] dilute to 1x) and stored at -80°C . For extraction of total RNA from heart tissue, 1 ml trizol (Invitrogen, 15596018) was added into each heart and crushed manually. Chloroform (200 μl) (Sigma-Aldrich, B9673-200 ml) was mixed into the crushed hearts and incubated for 3 min, at room temperature (RT). After incubation, hearts were centrifuged at 12,000 g, 15 min, supernatant was collected and 500 μl cold isopropanol (Thermo Fisher Scientific, A464-4) was added. The mixture was centrifuged again at 12,000 g, 10 min to pellet the RNA. The supernatant was discarded, and the pellet was washed in 500 μl of cold 75% ethanol, and centrifuged at 7500 g, 5 min. After repeating this step twice, the RNA pellet was air dried on ice, and then reconstituted using DNase-free water (Thermo Fisher Scientific, AM9937). RNA-seq was carried out as a paid service from the McGill University and Génome Québec Innovation Center, Canada. Briefly, paired-ends sequencing reads were clipped for adapter sequence, trimmed for minimum quality (Q30) in 3' and filtered for minimum length of 32 bp using Trimmomatic version 0.36 [53]. Surviving read pairs were aligned to the ENSEMBL release 83 Mus Musculus assembly using STAR version 2.5.3a [54] a two-pass approach. A gene-level count-based gene quantification against gene ENSEMBL annotations was performed using HT-seq count [55] in the *intersection-nonempty* mode. All of the above processing steps were accomplished through the GenPipes framework [56].

Gene expression analysis

Exploratory analysis was conducted using various functions and packages from R and the Bioconductor project [57]. Differential expression was conducted using both edgeR [58]. Terms from the Gene Ontology were tested for enrichment with the GOseq [59] R package.

Echocardiography

To assess cardiac function and morphometry, animals were assessed at baseline and 24 h post I-R, in a blinded manner under light anesthesia (1.5% isoflurane) using a GE Vivid 7 Dimension ultrasound machine (GE Medical Systems) with a i13 L14 MHz linear-array transducer. Measurements were taken at the mid-papillary level and used to determine left ventricular internal dimension at end-diastole (LVIDd), left ventricular internal dimension in systole (LVIDs), % ejection fraction (% EF) and % fractional shortening (% FS). A minimum of five images per mouse heart were analyzed.

Electron microscopy

Electron microscopy was performed in sham, I-R C57Bl/6 or CLOCK $\Delta 19/\Delta 19$ mice as previously described [60]. After 24 h of reperfusion, mice were anesthetized by intraperitoneal (i.p) injection of a combination of ketamine (100 mg/kg body weight) and xylazine (10 mg/kg body weight), euthanasia was performed by cervical dislocation followed by excision of the

heart. Briefly, hearts were excised and washed in phosphate buffer saline, four random areas of left ventricle between mid-region and apex were cut into small cubes and fixed in 2% w:v glutaraldehyde (Electron Microscopy Sciences, 16210). In order to study ultrastructural changes of the myocardium, tissues were osmicated, embedded in Epon (Electron Microscopy Sciences, 14960), stained with uranyl acetate (Electron Microscopy Sciences, 22409) and lead citrate (Electron Microscopy Sciences, 22410), as we previously reported [60]. Quantification of number and size of mitochondria was done using Image J software (NIH). Experiments were approved by animal care committee, University of Manitoba and carried out according to guidelines provided.

Quantitative real-time PCR (qPCR)

After 24 h of reperfusion, mice were anesthetized with isofluroane, sacrificed by cervical dislocation, hearts were excised, rinsed in PBS and stored at -80°C . For RNA extraction from cardiac myocytes, we used GenElute mammalian total RNA kit (Sigma Aldrich, RTN-350-1KT), according to manufacturer's instructions. cDNA was synthesized using iScript™ gDNA Clear cDNA Synthesis Kit (Bio-Rad, 172-5035), the quantitative Real-Time PCR reaction was amplified using iQ™ SYBR® Green Supermix (Bio-Rad, 14-222-777) with the following primers: *Clock*, *Atg7*, *Sqstm1*, *Rab7a*, *Tfeb* and housekeeping gene *Rpl32*, as explained previously [61], mitochondrial mass was quantified by real-time qPCR of *Tfam* and *Rpl32*. Primer sequences are presented in Table S2.

Western blot analysis

Mice were anesthetized with isoflurane at 24 h post-reperfusion, sacrificed by administration of 5% isoflurane and cervical dislocation, hearts and cells were lysed in RIPA buffer (1% triton x [Sigma-Aldrich, X100-1 L]-0.5 ml, 0.1% SDS-250 μl of 20% SDS, 140 mM NaCl-1.4 ml 5 M NaCl, 10 mM Tris-500 μl 1 M Tris pH 8, sodium deoxycholate-0.5 g, pH of RIPA 7.7) and protein was extracted and measured by bicinchoninic acid (BCA; Thermo Fisher Scientific, 23225). Lysate containing 20–30 μg of protein was resolved on denaturing SDS PAGE gels and then transferred to nitrocellulose membranes (Bio-Rad, 1620094). Membranes were probed with primary antibodies targeted against CLOCK (NEB, 5157S), OPA1 (Abcam, ab119865), MFN2 (Abcam, ab50838), BECN1/Beclin-1 (NEB, 3495S), ATG14 (Abcam, ab139727) or ACTA1/ACTIN (Sigma-Aldrich, A2172) at a 1:1000 dilution in TBS-T (5x 1 L [36.55 g NaCl, 15.5 g Tris, pH 7.4, 5 ml Tween-20 {VWR, Ac23336-0010}], dilute to x1.) overnight at 4°C , then incubated with secondary anti-murine or rabbit antibodies (as needed) conjugated to HRP (Cederlane, 715-035-150, 715-035-152). Bands were detected by enhanced ECL (GE Healthcare, CA89168-782) and visualized using an Amersham Imager 680 (GE Healthcare).

Cell culture and treatments

Cardiomyocytes were isolated from 1- to 2-day-old Sprague-Dawley rats, which were sacrificed by cervical dislocation. Hearts were excised and processed enzymatically to extract cardiomyocytes, which were then subjected to primary culture as previously reported [61]. Cultured cells were transfected with expression plasmids using Effectene reagent (Qiagen, Inc., 301427) or infected with adenovirus carrying the desired gene 24 h after plating under serum free DMEM (DMEM/F12 [Thermo Fisher Scientific, MT10092 CV]- 1 pack, NaHCO₃- 0.25 g, HEPES (Sigma-Aldrich, H3375-1 Kg) - 3.57 g, Na selenite (Sigma-Aldrich, S5261-100 G) -1 ml, transferrine (Sigma-Aldrich, T1408-500 MG) -1 ml, LiCl-1 ml, ascorbic acid (Sigma-Aldrich, A4034-100 G) -1 ml, insulin (Sigma-Aldrich, I0516-5 ml)-0.25 ml, T3 [L-Thyroxine-1 ml, gentamicin-1 ml] (Thermo Fisher Scientific, 15710072) conditions, as earlier described [61]). For hypoxia studies, cells were placed in an air-tight chamber continually gassed with 95% N₂, 5% CO₂, and pO₂ ≤ 5 mm Hg.

Plasmids, siRNAs and adenoviruses

The following plasmids were used: pCMV10/3xflag-Clock (Addgene, 47334; Takahashi lab), pCMV10/3xflag-Clock V315R (Addgene, 47342; Takahashi lab), pCMV10/3xflag-Clock L57E (Addgene, 47337; Takahashi lab), pCMV10/3xflag-Clock L57E/L113E/W284 (*Clock* 3xMut; Addgene, 47343; Takahashi lab). pcDNA4B-Flag *Clock* Δ19 was a gift from Carrie L Partch (University of California, Santa Cruz, California, USA) [62]. pcDNA flag HA plasmid (Addgene, 10792; Sellers lab) served as vehicle control for studies with plasmids. Cells were transfected for 18 h before being subjected to hypoxia. For CLOCK adenovirus studies, cells were infected for 24 h at a multiplicity of infection of 10–20 followed by hypoxia, empty cytomegalovirus (CMV) adenovirus (provided by Lorrie Kirshenbaum, University of Manitoba, Winnipeg, Manitoba, Canada [63]) served as control for our studies. The small interfering RNA (siRNA) against *Clock* was custom designed and synthesized by Invitrogen (see Supplementary materials, Table S2 for details). Briefly, cells were transfected with si*Clock* (60 nM), for 18 h, followed by media change and hypoxia for 18 h. Adenoviruses harboring shRNA against *Atg7* (sh*Atg7*), were generated as previously described [64] using the following hairpin-forming oligonucleotides: 5'-CGGTCAAAGGACAAAGTTAACATTCAAGA GATGTTAACTTTGTCCTTTGACCTTTTTA-3'.

Cell viability assay

Cardiomyocytes were incubated with the vital dyes calcein acetoxymethylester (Calcein-AM, 2 μM; Life Technologies, C3100MP) to visualize green cells (live) and ethidium homodimer-1 (2 μM) to visualize red cells (dead) by epifluorescence microscopy at x200 magnification, using Olympus AX-70 research fluorescence microscope.

Reactive oxygen species (ROS)

Cells were incubated with dihydroethidium (Invitrogen, D23107) (2.5 μM) for 30 min and visualized by epifluorescence microscopy using Olympus AX-70 fluorescence microscope. Increase in red fluorescence indicates increase in superoxide species production.

Mitochondrial membrane potential (ΔΨM)

Cells were incubated with tetra-methylrhodamine methyl ester perchlorate (TMRM; Thermo Fisher Scientific, T-668) (50 nM) and visualized by epifluorescence microscopy. Cell fluorescence intensity was measured by ImageJ software. In the case of TMRM, mitochondria with normal cells fluoresce bright red staining; however, red staining becomes diffuse or very light when mitochondrial membrane potential dissipates.

Mitochondrial respiration

Cardiomyocytes were cultured in 96-well plates and treated with CLOCK adenovirus or si*Clock* followed by 18 h hypoxia. Separate plate was treated the same way and left in normoxia for control. Both plates were assessed for mitochondrial oxygen consumption rate (OCR) on the same day, using XFe96 Cell Mito Stress Analyzer (Agilent). In brief, culture medium was changed 1 h before the assay to XF Base medium (Agilent, 102353–100), (pH 7.4) supplemented with 1 mM pyruvate (Thermo Fisher Scientific, 11360–070), and 10 mM D-glucose (Thermo Fisher Scientific, D16-500). Cells were then injected sequentially through ports in the Seahorse Flux Pak cartridges with oligomycin (1 μM; Sigma-Aldrich, O4876-5 MG), FCCP (2-[2-{4-(trifluoromethoxy)phenyl}hydrazinylidene]-propanedinitrile) (1 μM; Sigma-Aldrich, C2920), and rotenone (1 μM; Sigma-Aldrich, R8875-1 G) combined with antimycin (1 μM; Sigma-Aldrich, A8674-25 MG) as reported previously [65].

Mitochondrial morphology assay

Cardiomyocytes were plated on collagen from rat tails coated coverslips at a density of 4 × 10⁴, infected with CMV or CLOCK adenoviruses and subjected to hypoxia. After hypoxia, cells were washed with PBS and fixed with 4% paraformaldehyde (Electron Microscopy Science, 15710). Permeabilization was achieved with 0.5% Triton-x100 for 10 min, followed by blocking with 1% Triton X-100 + 2% bovine serum albumin (BSA; Roche, 10775835001) for 15 min. HSPD1/HSP60 antibody (Santa Cruz Biotechnology, sc-13115) was applied for mitochondrial staining in blocking solution for 1 h at RT, followed by incubation with donkey anti-mouse IgG secondary antibody, Alexa Fluor® 546 conjugate (Thermo Fisher Scientific, LSA10036) for 1 h, RT. Cells were counterstained with nuclear dye Hoechst (Thermo Fisher Scientific, 33342) and mounted with FluorSave™ Reagent (Millipore, 345789). Images were acquired by confocal microscopy (Carl Zeiss Axio Observer SD) using the magnification 630× and Zen Software. For analysis, ImageJ software was used to calculate form factor (FF: perimeter² /

4 π -Area), a measure of length and branching corresponding to a circular mitochondrion; values increase with mitochondrial elongation, as previously described [66].

Autophagic flux

To assess autophagy in cardiomyocytes, cells were plated on coverslips at a density of 4×10^4 . On the next day, cells were co-infected with adenoviruses encoding green fluorescent protein (GFP)-fused LC3 (provided by Junichi Sadoshima, Rutgers University, New Jersey, USA [67]), CMV or CLOCK (constructed by Lorrie Kirshenbaum, University of Manitoba, Winnipeg, Manitoba, Canada). Chloroquine treatment was used as a positive control for autophagic flux. After 18 h of hypoxia, cells were fixed with 4% paraformaldehyde (Electron Microscopy Science, 15710), and washed with PBS. Prior to imaging, slides were mounted with FluorSave™ Reagent (Millipore, 345789), images were acquired by confocal microscopy (Carl Zeiss Axio Observer SD) using the magnification 630 \times and Zen Software (Carl Zeiss) [68]. For analysis, the number of GFP dots was determined by manual counting of fluorescent puncta from three different myocyte preparations with a 60 \times objective. The number of dots per cell was obtained by dividing the total number of dots by the number cells.

MitoKeima staining

Keima with mitochondrial localization signaling (MitoKeima) acts as a mitochondrial localized pH indicator protein, as previously described [30]. Cardiomyocytes were transfected with *Clock* plasmids or vector control pcDNA HA flag in addition to infection with MitoKeima adenovirus (provided by Junichi Sadoshima, Rutgers University, New Jersey, USA [69]). Following hypoxia, cells were washed with PBS and fixed with 4% paraformaldehyde (Electron Microscopy Science, 15710). Cells were mounted with FluorSave™ Reagent (Millipore, 345789) and images acquired by confocal microscopy (Carl Zeiss Axio Observer SD) using the magnification 63 \times and Zen Software (Carl Zeiss). Mitophagy was quantified using Zeiss ZEN Blue software measuring the fluorescence signal ratio 560/440 nm and size of MitoKeima puncta. The higher 560/440 signal ratio (red/yellow color) indicates mitochondria that have fused with lysosomes (acidic pH), lower 560/440 signal ratio (green color) indicative of complete mitochondrial clearance. The size of puncta was measured by delineating the five largest puncta in each image and the fold-change in area was calculated by averaging 3–5 images from each condition and normalized to control, assigned the value of one. In each experimental model, all imaging parameters remain the same for all data acquisition.

Luciferase assay

Cells were transfected with a *Tfeb* luciferase reporter construct designated (TFEBluc), as previously described [70]. Luciferase activity was normalized to β -galactosidase activity to control for differences in transfection efficiency and data are expressed as relative light units.

Statistical analysis

Data are expressed as average \pm SEM. Multiple comparisons between groups were determined by one-way ANOVA. Tukey's post hoc test was used to determine differences among groups. The unpaired two tailed Student's *t*-test was used to compare mean differences between two groups. Differences were considered to be statistically significant to a level of $*p < 0.05$ or $**p < 0.01$. In all studies, data were obtained from at least $n = 3$ –6 independent myocyte isolations for each condition tested.

Acknowledgments

We are grateful to Hongying Gang, Floribeth Aguilar, and Raya Margulets for technical assistance and critical comments on the manuscript. The Canadian Center for Computational Genomics (C3G) is a Genomics Technology Platform (GTP) which is supported by the Canadian Government through Genome Canada.

Disclosure statement

The authors declare no competing interests.

Funding

This work was supported by a Foundation grant to L.A.K from the Canadian Institute for Health Research (CIHR) and St. Boniface Hospital Research Foundation, and a project grant to T.A.M. from CIHR. T.A.M. is a Career Investigator of the Heart and Stroke Foundation of Canada. L.A.K. holds a Canada Research Chair in Molecular Cardiology; I.R.N. holds a Post-doctoral Fellowship from the CIHR

References

- [1] Ashrafian H, Frenneaux MP, Opie LH. Metabolic mechanisms in heart failure. *Circulation*. 2007;116:434–448.
- [2] Balaban RS, Nemoto S, Finkel T. Mitochondria, oxidants, and aging. *Cell*. 2005;120:483–495.
- [3] Reznick RM, Zong H, Li J, et al. Aging-associated reductions in AMP-activated protein kinase activity and mitochondrial biogenesis. *Cell Metab*. 2007;5:151–156.
- [4] Zid BM, Rogers AN, Katewa SD, et al. 4E-BP extends lifespan upon dietary restriction by enhancing mitochondrial activity in drosophila. *Cell*. 2009;139:149–160.
- [5] Petrie JR, Guzik TJ, Touyz RM. Diabetes, hypertension, and cardiovascular disease: clinical insights and vascular mechanisms. *Can J Cardiol*. 2018;34:575–584.
- [6] Ikeda Y, Sciarretta S, Nagarajan N, et al. New insights into the role of mitochondrial dynamics and autophagy during oxidative stress and aging in the heart. *Oxid Med Cell Longev*. 2014;2014. DOI:10.1155/2014/210934
- [7] Rabinovich-Nikitin I, Lieberman B, Martino TA, et al. Circadian-regulated cell death in cardiovascular diseases. *Circulation*. 2019;139:965–980.
- [8] Adamovich Y, Ladeuix B, Golik M, et al. Rhythmic oxygen levels reset circadian clocks through HIF1 α . *Cell Metab*. 2017;25:93–101.
- [9] Portaluppi F, Tiseo R, Smolensky MH, et al. Circadian rhythms and cardiovascular health. *Sleep Med Rev*. 2012;16:151–166.
- [10] Martino TA, Young ME. Influence of the cardiomyocyte circadian clock on cardiac physiology and pathophysiology. *J Biol Rhythms*. 2015;30:183–205.

- [11] Lowrey PL, Takahashi JS. Genetics of circadian rhythms in Mammalian model organisms. *Adv Genet.* 2011;74:175–230
- [12] Bray MS, Shaw CA, Moore MWS, et al. Disruption of the circadian clock within the cardiomyocyte influences myocardial contractile function, metabolism, and gene expression. *Am J Physiol Circ Physiol.* 2008;294:H1036–47.
- [13] Durgan DJ, Hotze MA, Tomlin TM, et al. The intrinsic circadian clock within the cardiomyocyte. *Am J Physiol Circ Physiol.* 2005;289:H1530–41.
- [14] Alibhai FJ, LaMarre J, Reitz CJ, et al. Disrupting the key circadian regulator CLOCK leads to age-dependent cardiovascular disease. *J Mol Cell Cardiol.* 2017;105:24–37.
- [15] Lefta M, Campbell KS, Feng H-Z, et al. Development of dilated cardiomyopathy in Bmal1-deficient mice. *Am J Physiol Circ Physiol.* 2012;303:H475–85.
- [16] Baron KG, Reid KJ. Circadian misalignment and health. *Int Rev Psychiatry.* 2014;26:139–154.
- [17] Alibhai FJ, Tsimakouridze EV, Reitz CJ, et al. Consequences of circadian and sleep disturbances for the cardiovascular system. *Can J Cardiol.* 2015;31:860–872.
- [18] Reitz CJ, Martino TA. Disruption of circadian rhythms and sleep on critical illness and the impact on cardiovascular events. *Curr Pharm Des.* 2015;21:3505–3511.
- [19] Durgan DJ, Young ME. The cardiomyocyte circadian clock: emerging roles in health and disease. *Circ Res.* 2010;106:647–658.
- [20] Vitaterna MH, King DP, Chang AM, et al. Mutagenesis and mapping of a mouse gene, clock, essential for circadian behavior. *Science.* 1994;264:719–725.
- [21] Bertolucci C, Cavallari N, Colognesi I, et al. Evidence for an overlapping role of CLOCK and NPAS2 transcription factors in liver circadian oscillators. *Mol Cell Biol.* 2008;28:3070–3075.
- [22] Debruyne JP. Oscillating perceptions: the ups and downs of the CLOCK protein in the mouse circadian system. *J Genet.* 2008;87:437–446.
- [23] Debruyne JP, Noton E, Lambert CM, et al. Mouse CLOCK is not required for circadian oscillator function. *Neuron.* 2006;50:465–477.
- [24] Duong ATH, Reitz CJ, Louth EL, et al. The Clock mechanism influences neurobiology and adaptations to heart failure in clock $\Delta 19/\Delta 19$ mice with implications for circadian medicine. *Sci Rep.* 2019;9. DOI:10.1038/s41598-019-41469-7
- [25] Asher G, Schibler U. Crosstalk between components of circadian and metabolic cycles in mammals. *Cell Metab.* 2011;13:125–137.
- [26] Bass J, Takahashi JS. Circadian integration of metabolism and energetics. *Science.* 2010;330:1349–1354.
- [27] Zhang EE, Kay SA. Clocks not winding down: unravelling circadian networks. *Nat Rev Mol Cell Biol.* 2010;11:764–776.
- [28] Panda S, Hogenesch JB, Kay SA. Circadian rhythms from flies to human. *Nature.* 2002;417:329–335.
- [29] Muñoz E, Brewer M, Baler R. Circadian transcription: thinking outside the E-Box. *J Biol Chem.* 2002;277:36009–36017.
- [30] Katayama H, Kogure T, Mizushima N, et al. A sensitive and quantitative technique for detecting autophagic events based on lysosomal delivery. *Chem Biol.* 2011;18:1042–1052.
- [31] Gang H, Dhingra R, Lin J, et al. PDK2-mediated alternative splicing switches Bnip3 from cell death to cell survival. *J Cell Biol.* 2015;210:1101–1115.
- [32] Huang N, Chelliah Y, Shan Y, et al. Crystal structure of the heterodimeric CLOCK:BMAL1 transcriptional activator complex. *Science.* 2012;337:189–194.
- [33] Mistry P, Duong A, Kirshenbaum L, et al. Cardiac Clocks and preclinical translation. *Heart Fail Clin.* 2017;13:657–672.
- [34] Kubli DA, Gustafsson ÅB. Mitochondria and mitophagy: the yin and yang of cell death control. *Circ Res.* 2012;111:1208–1221.
- [35] Dorn GW, Kitsis RN. The mitochondrial dynamism-mitophagy-cell death interactome: multiple roles performed by members of a mitochondrial molecular ensemble. *Circ Res.* 2015;116:167–182.
- [36] Tong M, Saito T, Zhai P, et al. Mitophagy is essential for maintaining cardiac function during high fat diet-induced diabetic cardiomyopathy. *Circ Res.* 2019;CIRCRESAHA.118.314607.
- [37] Shirakabe A, Zhai P, Ikeda Y, et al. Drp1-dependent mitochondrial autophagy plays a protective role against pressure overload-induced mitochondrial dysfunction and heart failure. *Circulation.* 2016;133:1249–1263.
- [38] Hamacher-Brady A, Brady NR, Logue SE, et al. Response to myocardial ischemia/reperfusion injury involves Bnip3 and autophagy. *Cell Death Differ.* 2007;14:146–157.
- [39] De Lazzari F, Bisaglia M, Zordan MA, et al. Circadian rhythm abnormalities in parkinson's disease from humans to flies and back. *Int J Mol Sci.* 2018;19. DOI:10.3390/ijms19123911
- [40] Pascual F, Coleman RA. Fuel availability and fate in cardiac metabolism: a tale of two substrates. *Biochim Biophys Acta - Mol Cell Biol Lipids.* 2016;1861:1425–1433.
- [41] Liesa M, Shirihai OS. Mitochondrial dynamics in the regulation of nutrient utilization and energy expenditure. *Cell Metab.* 2013;17:491–506.
- [42] Youle RJ, Van Der Bliek AM. Mitochondrial fission, fusion, and stress. *Science.* 2012;337:1062–1065.
- [43] Podobed P, Pyle WG, Ackloo S, et al. The day/night proteome in the murine heart. *Am J Physiol Integr Comp Physiol.* 2014;307:R121–37.
- [44] Podobed PS, Alibhai FJ, Chow CW, et al. Circadian regulation of myocardial sarcomeric Titin-cap (Tcap, telethonin): identification of cardiac clock-controlled genes using open access bioinformatics data. *PLoS One.* 2014;9:e104907.
- [45] Tsimakouridze EV, Straume M, Podobed PS, et al. Chronomics of pressure overload-induced cardiac hypertrophy in mice reveals altered day night gene expression and biomarkers of heart disease. *Chronobiol Int.* 2012;29:810–821.
- [46] Martino T, Arab S, Straume M, et al. Day/night rhythms in gene expression of the normal murine heart. *J Mol Med.* 2004;82:256–264.
- [47] Storch KF, Lipan O, Leykin I, et al. Extensive and divergent circadian gene expression in liver and heart. *Nature.* 2002;417:78–83.
- [48] Koike N, Yoo SH, Huang HC, et al. Transcriptional architecture and chromatin landscape of the core circadian clock in mammals. *Science.* 2012;338:349–354.
- [49] Jacobi D, Liu S, Burkewitz K, et al. Hepatic Bmal1 regulates rhythmic mitochondrial dynamics and promotes metabolic fitness. *Cell Metab.* 2015;22:709–720.
- [50] Li E, Li X, Huang J, et al. BMAL1 regulates mitochondrial fission and mitophagy through mitochondrial protein BNIP3 and is critical in the development of dilated cardiomyopathy. *Protein Cell.* 2020;11:661–679.
- [51] Scheer FAJL, Hilton MF, Mantzoros CS, et al. Adverse metabolic and cardiovascular consequences of circadian misalignment. *Proc Natl Acad Sci.* 2009;106:4453–4458.
- [52] Alibhai FJ, Tsimakouridze EV, Chinnappareddy N, et al. Short-term disruption of diurnal rhythms after murine myocardial infarction adversely affects long-term myocardial structure and function. *Circ Res.* 2014;114:1713–1722.
- [53] Bolger AM, Lohse M, Usadel B. Trimmomatic: a flexible trimmer for Illumina sequence data. *Bioinformatics.* 2014;30:2114–2120.
- [54] Dobin A, Davis CA, Schlesinger F, et al. STAR: ultrafast universal RNA-seq aligner. *Bioinformatics.* 2013;29:15–21.
- [55] Anders S, Pyl PT, Huber W. HTSeq-A Python framework to work with high-throughput sequencing data. *Bioinformatics.* 2015;31:166–169.
- [56] Bourgey M, Dali R, Eveleigh R, et al. GenPipes: an open-source framework for distributed and scalable genomic analyses. *Gigascience.* 2019;1(8(6)):pii: giz037.
- [57] Huber W, Carey VJ, Gentleman R, et al. Orchestrating high-throughput genomic analysis with bioconductor. *Nat Methods.* 2015;12:115–121.

- [58] Robinson MD, McCarthy DJ, Smyth GK. edgeR: a bioconductor package for differential expression analysis of digital gene expression data. *Bioinformatics*. 2009;26:139–140.
- [59] Young MD, Wakefield MJ, Smyth GK, et al. Gene ontology analysis for RNA-seq: accounting for selection bias. *Genome Biol*. 2010;11:R14.
- [60] Dhingra R, Guberman M, Rabinovich-Nikitin I, et al. Impaired NF- κ B signalling underlies cyclophilin D-mediated mitochondrial permeability transition pore opening in doxorubicin cardiomyopathy. *Cardiovasc Res*. 2019;116:1161–1174.
- [61] Gang H, Hai Y, Dhingra R, et al. A novel hypoxia-inducible spliced variant of mitochondrial death gene Bnip3 promotes survival of ventricular myocytes. *Circ Res*. 2011;108:1084–1092.
- [62] Michael AK, Harvey SL, Sammons PJ, et al. Cancer/testis antigen PASD1 silences the circadian Clock. *Mol Cell*. 2014;58:743–754.
- [63] Kirshenbaum LA, MacLellan WR, Mazur W, et al. Highly efficient gene transfer into adult ventricular myocytes by recombinant adenovirus. *J Clin Invest*. 1993;92:381–387.
- [64] Saito T, Nah J, Oka SI, et al. An alternative mitophagy pathway mediated by Rab9 protects the heart against ischemia. *J Clin Invest*. 2019;129:802–819.
- [65] Roy Chowdhury SK, Smith DR, Saleh A, et al. Impaired adenosine monophosphate-activated protein kinase signalling in dorsal root ganglia neurons is linked to mitochondrial dysfunction and peripheral neuropathy in diabetes. *Brain*. 2012;135:1751–1766.
- [66] Sassone F, Margulets V, Maraschi A, et al. Bcl-2/adenovirus E1B 19-kDa interacting protein (BNip3) has a key role in the mitochondrial dysfunction induced by mutant huntingtin. *Hum Mol Genet*. 2015;24:6530–6539.
- [67] Hariharan N, Zhai P, Sadoshima J. Oxidative stress stimulates autophagic flux during ischemia/reperfusion. *Antioxid Redox Signal*. 2011;14:2179–2190.
- [68] Sciarretta S, Hariharan N, Monden Y, Zablocki D, Sadoshima J. Is autophagy in response to ischemia and reperfusion protective or detrimental for the heart?. *Pediatr Cardiol*. 2011;32(3):275–281.
- [69] Shirakabe A, Fritzky L, Saito T, et al. Evaluating mitochondrial autophagy in the mouse heart. *J Mol Cell Cardiol*. 2016;92:134–139.
- [70] Dhingra R, Gang H, Wang Y, et al. Bidirectional regulation of nuclear factor- κ B and mammalian target of rapamycin signaling functionally links bnip3 gene repression and cell survival of ventricular myocytes. *Circ Hear Fail*. 2013;6:335–343.